A Review of Faults and Crustal Structure in the San Francisco Bay Area as Revealed by Seismic Studies: 1991–97

By Tom Parsons, Jill McCarthy, Patrick E. Hart, John A. Hole, Jon Childs, David H. Oppenheimer, and Mary Lou Zoback

CONTENTS

Abstract

This report summarizes and integrates the results from various seismic experiments conducted in the San Francisco Bay region. Three marine deep seismic-reflection surveys, two local-earthquake tomography studies, and multiple, focused high-resolution seismic-reflection experiments were aimed at resolving the structure of the strike-slip faults in the Pacific-North American Plate boundary zone. The primary conclusion from these studies is that the major strike-slip faults in the bay region cut through the entire crust at high angles (60º–80º). This conclusion implies that horizontal shear in the midcrust or lower crust plays a minimal role in accommodating the right-lateral strain that was proposed in several tectonic models. Among the major faults in the San Francisco Bay region, throughgoing faults identified by marine data are the Kirby Hills Fault in the eastern San Francisco Bay region (dipping ~80º NE. in the lower crust), the Hayward Fault (dipping ~70º SW. in the lower crust), and the San Andreas Fault (dipping ~60º NE. in the lower crust). Strong lateral seismic-velocity contrasts across major right-lateral strike-slip faults are revealed by a three-dimensional tomography model in much of the upper crust to midcrust of the San Francisco Bay region. These cross fault velocity contrasts affect determinations of earthquake focal mechanisms, hypocenter locations, and simulated strong ground motion because seismic energy can be refracted laterally along such velocity boundaries. Localized tomography on the San Francisco peninsula indicates that the Pilarcitos Fault, paralleling the San Andreas Fault, is high angle and thus probably not an active thrust fault, as has been proposed. Most high-amplitude reflections in the lower crust are now recognized as reflecting from the dipping Hayward and San Andreas Faults. When these dipping reflections are accounted for, the remaining reflective texture of the lower crust is weak and highly discontinuous.

Introduction

Between 1991 and 1998, the U.S. Geological Survey (USGS) operated a project designed to augment earthquake-hazard studies in urban central California by focusing on earthquake sources and ground response at submerged and coastal sites. This report summarizes efforts within this project to identify and map fault structures by using seismic techniques. When the project was initiated, there was vigorous debate whether the major right-lateral faults connected to a low-angle detachment fault below seismogenic depths. Various proposals suggested that this low-angle detachment fault linked strain between the vertical strike-slip faults. Thus,

much of the initial focus of active-source marine seismic-data acquisition was aimed at resolving deep crustal structure. As the project matured, the goals of the USGS moved somewhat away from basic science toward more applied studies, and seismic projects began to be directed at shallow structure and specific faults. Here, we summarize and integrate most of the results from active- and passive-source seismic studies in the San Francisco Bay area conducted by, or in association with, the USGS and summarize what was learned about some of the major fault zones and associated crustal structures. Additional studies were conducted on the Golden Gate platform by Bruns and others (this volume), and Hart and others (this volume) discuss all the marine seismic data acquisition in the San Francisco Bay area by the USGS between 1991 and 1998.

Tectonic Setting and Geology of the San Francisco Bay Region

The San Francisco Bay region occupies a broad part of the San Andreas Fault system; the San Andreas Fault splays from a single fault just south of the region into several segments that cross east and west of the bay. A complex pattern of bending strike-slip faults and related accommodating thrust and normal faults is arrayed across the bay region; many of these faults pose a significant seismic hazard as evidenced by the *M*=7.1 1989 Loma Prieta, *M*=7.7 1906 San Francisco (Thatcher, 1975), and *M*~6.8 1868 Hayward (Bakun, 1999) earthquakes. Right-lateral shear takes place on several subparallel strike-slip faults (fig. 1), such as the San Andreas, Hayward, and Calaveras Faults, which together accommodate about 4 cm/yr of relative motion between the Pacific and North American Plates (for example, DeMets and others, 1990; Lisowski and others, 1991; Kelson and others, 1992). The San Andreas Fault on the San Francisco peninsula is a relatively young feature that initiated about 3.3–1.3 Ma and has undergone ~23 km of right-lateral offset (Cummings, 1968; Addicott, 1969; Taylor and others, 1980; Hall, 1984, Hall and Wright, 1993; Hall and others, 1996). Faults east of San Francisco Bay (that is, the Calaveras and Hayward Faults) have cumulatively accommodated as much as 160 to 170 km of right-lateral strain (for example, McLaughlin and others, 1996)

Like much of coastal California, the San Francisco Bay region is underlain primarily by the Late Mesozoic/Early Tertiary Franciscan Complex of accreted origin, an assemblage that contains fragments of oceanic crust, pelagic sedimentary rocks, and continental sandstone and shale mixed together in a melange in some places and occurring as coherent units in others (Page, 1992). These rocks were emplaced during the long-term phase of oblique to head-on subduction that occurred along the California margin, and many were subsequently translated along the coast during oblique subduction and when strike-slip motion supplanted subduction during Tertiary time (Blake, 1984). In general, Cretaceous granite of the Salinia terrane is exposed west of the San Andreas Fault (fig. 1; see Ross, 1978), although the Pilarcitos Fault marks that boundary on the San Francisco peninsula.

Regionally, earthquakes are observed at ~0- to 15-km depth (Hill and others, 1990), and their distribution indicates that the major strike-slip faults are near vertical in the seismogenic crust. Beneath about 15- to 20-km depth, the major strike-slip faults of the San Francisco Bay region may strain aseismically (Olson and Lindh, 1985; Dewey and others, 1989; Hill and others, 1990; Lisowski and others, 1991; Olson and Zoback, 1992). The absence of earthquake hypocenters beneath that depth has left many unresolved questions about the relations among the steeply dipping right-lateral transform faults that make up the San Andreas Fault zone in the San Francisco Bay region (fig. 1) within the ductile regime. Various tectonic models for plate interactions in the bay region (for example, Furlong and others, 1989; Furlong, 1993; Page and Brocher, 1993; Brocher and others, 1994; Jones and others, 1994; Bohannon and Parsons, 1995) suggest that horizontal shear in the deep crust drives or, at least, accommodates the strain expressed at the surface. Many researchers have proposed that a low-angle detachment fault between 15- and 20-km depth could link slip between the San Andreas and Hayward Faults (fig. 2; see Furlong, 1993; Brocher and others, 1994; Bürgmann, 1997).

Onland Crustal Seismic Experiments in the San Francisco Bay Region Since 1991

We briefly summarize seismic-data acquisition conducted on land since 1991. Marine acquisition, including the Bay Area Seismic Imaging eXperiment (BASIX) studies, during this period is discussed by Hart and others (this volume).

Land Explosive-Source Studies, 1991–93

In 1991 and 1993, chemical explosions were detonated along the San Andreas, Calaveras, and Hayward Faults to study the rupture zone of the *M*=7.1 1989 Loma Prieta, Calif., earthquake and to measure seismic travelpaths through the crust (Catchings and Kohler, 1996). Six explosive sources and about 200 recorders were used to construct a velocity model of the crust along the San Francisco peninsula. Key observations were that the crust thins significantly from about 30 km near Loma Prieta to about 22 km beneath San Francisco and that earthquake shaking in San Francisco caused by the 1989 earthquake may have been augmented by reflected energy from the Moho (Catchings and Kohler, 1996).

Land-Array and Explosive-Source Studies in 1995

Beginning in January 1995, 31 Reftek seismographs were installed in an array spanning the San Francisco peninsula and the San Andreas and Pilarcitos Faults (fig. 3; see Parsons and Zoback, 1997; Parsons, 1998). The instruments were spaced

about 1 to 3 km apart in any given direction and recorded continuously for 6 months. Most of the 23 seismometers were short-period (4.5 Hz) three-component sensors, 7 were intermediate-period (1 Hz) three-component sensors, and 1 was a downhole broadband sensor. These instruments each recorded an average of 105 local earthquakes (M=1.0–3.0) from January through July 1995. In April 1995, marine airgun sources were recorded (for a complete description of the marine experiments, see Hart and others, this volume). In June 1995, 11 chemical explosions (125–500 kg) were detonated inside and outside the network (fig. 3). The explosive sources were recorded both on the 31 Reftek seismographs and on 183 Seismic Group Recorders (SGRs) that were deployed along a southwest-to-northeast line across the Pilarcitos and San Andreas Faults (fig. 3). The SGRs were deployed at 50-m spacing in a fixed array that recorded 7 inline shots spaced between 1 and 5 km apart and 4 fanshots located 5 to 20 km both north and south of the recording profile. The closely spaced SGRs enabled us to generate a higher resolution two-dimensional velocity model of the uppermost 2 km of crust across the Pilarcitos Fault and to observe high-amplitude reflections from deep in the crust.

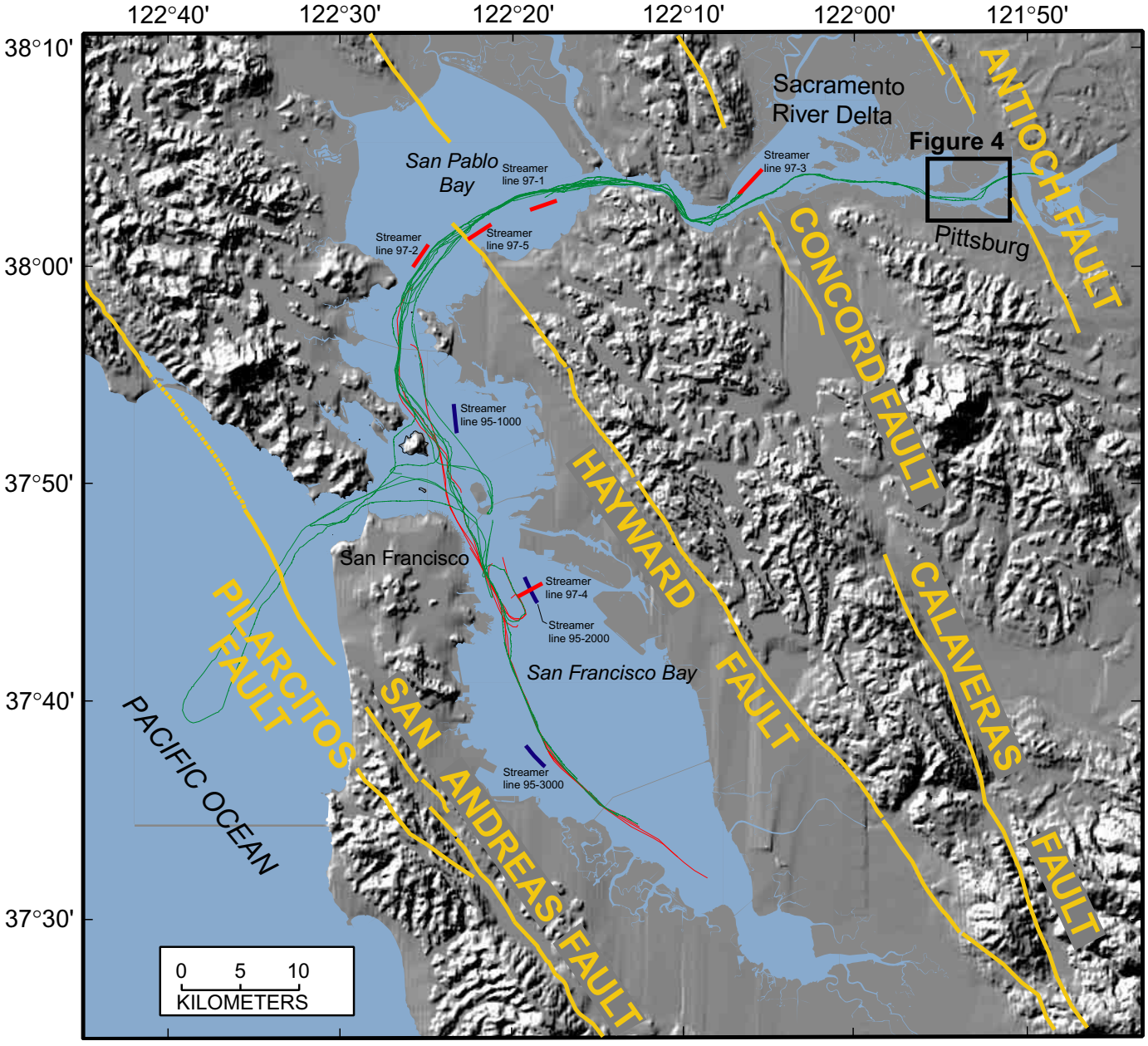

Figure 1.—San Francisco Bay region, showing locations of major faults and seismic-reflection profiles. Large airgun sources were deployed along green lines, and receiver cables as shown by short red and blue lines. In addition, many higher-resolution seismic-reflection profiles were gathered throughout the region.

Results from Seismic Experiments in the San Francisco Bay Region

Here, we summarize our enhanced view into the crust of the San Francisco Bay region as provided by several imaging techniques. We present previously unpublished studies and expanded discussion, integration, and support of some published results. Much of the investigation and imaging was concentrated on active faults, either on their structure in the seismogenic zone (~3–15-km depth) or on their relations and connectivity in the lower crust beneath seismogenic depths. Some higher-resolution, shallower data were acquired for previously unknown or poorly known faults. We present the studies and principal results in chronological order, followed by a discussion and integration of the results.

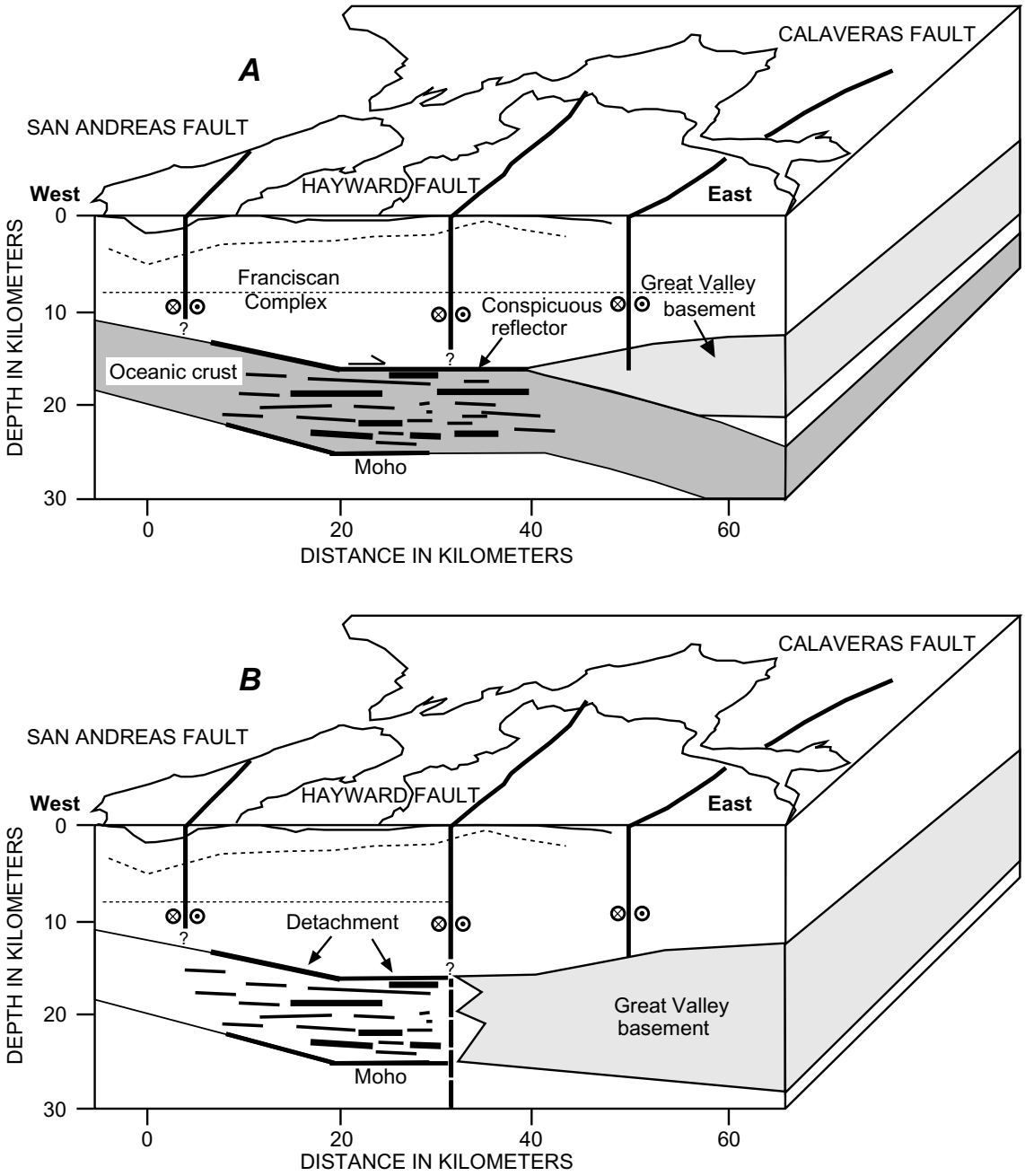

Figure 2.—Block diagrams of the San Francisco Bay region (fig. 1), illustrating two candidate models for deep configuration of bay-region faults. Either faults (*A*) persist to midcrustal depths where, at base of seismicity, they terminate into a low-angle or detachment fault (for example Furlong and others, 1989; Furlong, 1993; Page and Brocher, 1993; Brocher and others, 1994; Jones and others, 1994); or (*B*) they cut through whole crust.

1991: BASIX–1, the Kirby Hills Fault Zone

Marine seismic-reflection data acquisition in San Francisco Bay poses severe challenges because of the shallow water depth, strong currents, and heavy shipping traffic. Not all of these problems were overcome during the first experiment in 1991, and data quality was poor in many places. However, east of San Francisco Bay in the Sacramento River delta (fig. 1), good-quality data were acquired and processed that confirmed the existence of the Kirby Hills Fault zone, which, along with the Antioch Fault, represents the easternmost segment of the San Andreas Fault system at the latitude of the Sacramento River. This feature is a reactivated structure that began its history as a normal fault during the Eocene (Krug and others, 1992; McKevett, 1992). Presently, the Kirby Hills Fault zone is a strike-slip fault dipping 80º–85º E. The fault is seismically active and is characterized by some of the deepest earthquakes recorded south of the Mendocino triple junction in northern California (Hill and others, 1990).

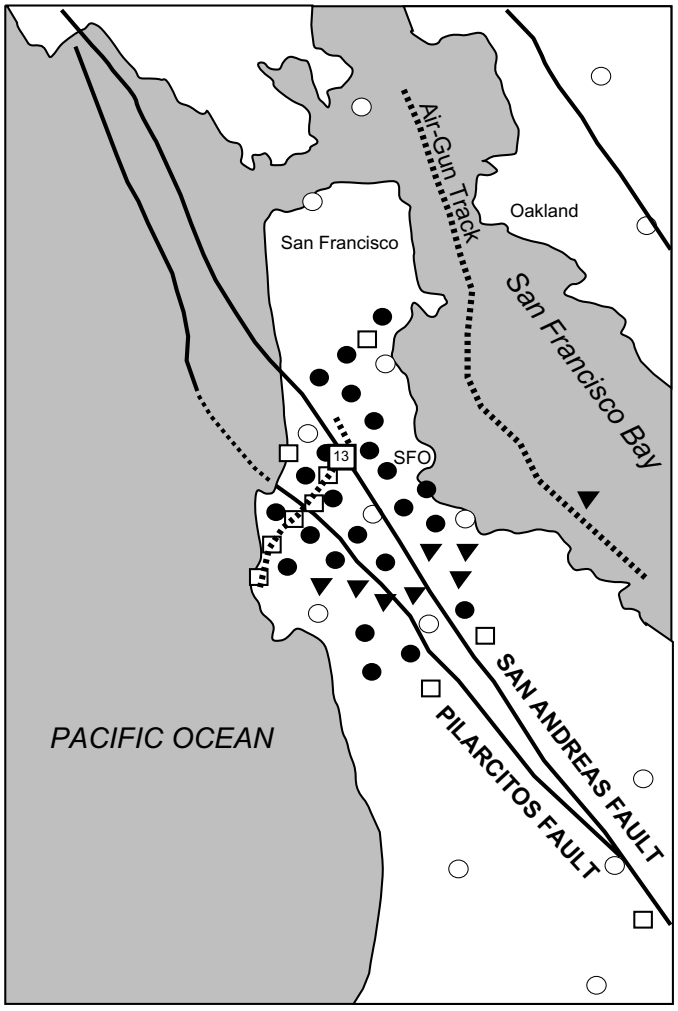

Figure 3.—Sketch map of the San Francisco Bay region (fig. 1), showing location of land-based San Francisco peninsula seismic experiment. Dots and triangles, stations in temporary (6 month) seismic network; circles, permanent stations in the Northern California Seismic Network (Calnet). Dashed line in San Francisco Bay denotes approximate trackline for airgun shots recorded by Calnet (see fig. 1). Squares, chemical-explosive shotpoints (box labeled "13" is gather shown in fig. 13); dashed line on peninsula, high-resolution refraction and deep reflection profile.

Various acoustic tools have been used to image the subsurface geometry of faults at different depths in the Earth's crust. A tradeoff exists between subsurface resolution and depth of source penetration, with lower-resolution but more powerful sources reaching deeper into the crust. When shallow and intermediate-depth acoustic images are combined with the information derived from deep earthquake activity, the position of the Kirby Hills Fault can be mapped down to the base of the crust. Such control is rare and provides important constraints on the physical properties and structural architecture of the midcrust and lower crust underlying the California Coast Ranges. Here, we present acoustic images that collectively define the subsurface geometry of the Kirby Hills Fault zone near Pittsburg (figs. 1, 4) and document that this structure cuts the entire crust down to at least 28-km depth.

Ultra-High-Resolution Images of the Kirby Hills Fault Zone

The ultra-high-resolution data provide images of deformed and folded sedimentary rocks in the uppermost 30 m of crust. Two windows from a single ultra-high-resolution profile within the 1-km-wide Kirby Hills fault zone are shown in figure 5. The eastern ultra-high-resolution profile (fig. 5*A*) reveals a conspicuous unconformity (reflector B) in the shallow near-surface, approximately 15 m subbottom. Beneath this unconformity, strata dip approximately 5º–10º W., whereas above the discontinuity, channel-fill deposits are nearly flat lying.

To the west (fig. 5*B*), the unconformity is broadly warped and uplifted. The antiform breaches the surface near the confluence of the Sacramento and San Joaquin Rivers, just opposite the town of Pittsburg (figs. 1, 4). Deformation of the river floor confirms that the Kirby Hills Fault zone is an active feature.

Acoustic Images of the Uppermost 75 m of the Crust Across the Kirby Hills Fault Zone

In the vicinity of the Kirby Hills Fault zone, a high-resolution source provides vivid images of the uppermost 75 m of crust. Two representative profiles are shown in figure 6, each of which displays the same three principal features identified on the ultra-high-resolution profiles: (1) an upper series of flat-lying to gently dipping sedimentary strata, (2) a conspicuous angular unconformity, and (3) a deeper series of 5º–10º-W.-dipping strata that terminates abruptly at the unconformity. On the high-resolution profiles, the upper sedimentary strata display a slight westward dip and onlap the underlying angular unconformity. The unconformity itself is warped and folded and occurs at 5- to 35-m depth. The

undulation of the unconformity suggests ongoing deformation associated with the fault zone.

Intermediate-Resolution Images of the Uppermost 2 km of Crust Across the Kirby Hills Fault Zone

Small-airgun, multichannel seismic-reflection profiles were acquired to provide a deeper picture of the crustal structure across the deformation zone identified in the higher-resolution profiles. Two of the six profiles acquired (fig. 7) provide high-quality images of the crustal structure in the uppermost 1 km of crust in the vicinity of Pittsburg (fig. 4). These two profiles document an abrupt deformational front, east of which reflections are abruptly folded in an eastward-vergent geometry. This folding extends to at least 600-m depth, but no fault-plane reflections are evident. Without clear images of the fault plane, it is difficult to constrain the style of faulting, whether fault-bend folding or fault-propagation folding. East of the zone of folding, small-airgun, multichannel seismic-reflection profiles show a conspicuous reflection at ~400-m subbottom (reflector C, fig. 7). This event corresponds to a second, deeper unconformity, as discussed below. The data indicate folding and faulting that extends down to 4.5-km depth. The conspicuous unconformity imaged at ~0.4-s two-way traveltime (reflector C) is independent of the unconformity imaged by higher-resolution techniques.

Seismic Images of the Uppermost 6 to 9 km of Crust Across the Kirby Hills Fault Zone

A lower-frequency multichannel seismic-reflection profile complements the higher-resolution, shallower-penetration images and allows us to image the Kirby Hills Fault zone down to 6- to 9-km depths (fig. 8). The multichannel seismic source used to investigate the Kirby Hills Fault zone had a dominant frequency of 10 to 20 Hz and consisted of a 12-element, 13.8-MPa, 95.5-L tuned-airgun array towed from the USGS research vessel *S.P. Lee*. The airguns were towed at an average water depth of 7.6 m and were fired at a 50-m interval (see Hart and others, this volume).

A reflection at 1-s two-way traveltime is believed to correspond to the top of the Eocene Domengine Formation, as mapped by Krug and others (1992). Multichannel seismic images show upward warping and deformation within the fault zone in the uppermost 2 to 4 km of crust. These different data sets show a strong vertical alignment of deformation. Thus, even though the near-vertical fault is not imaged, the location of the fault can be construed by identifying the zone of folded and offset strata at ever-increasing depths in the crust. In the lower crust, earthquakes are used to constrain the location of the Kirby Hills Fault.

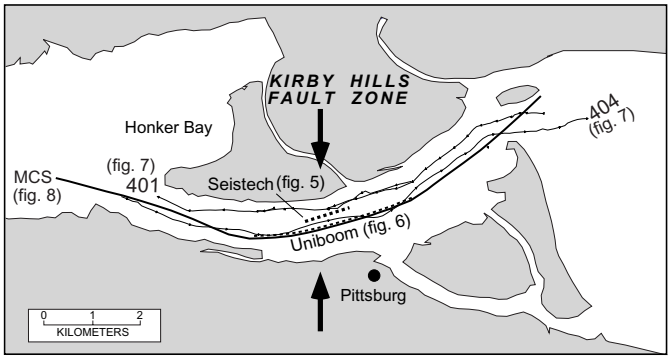

Figure 4.—Study area of the Kirby Hills Fault zone (see fig. 1 for location). Marine profiles of various resolutions shown in figures 5 through 8 were gathered along heavy black line. Fault zone is ~1 km wide and is centered over arrows.

Seismicity in the Vicinity of the Kirby Hills Fault Zone

Faulting and deformation along the Kirby Hills Fault zone is associated with unusually deep seismicity, ranging from 15- to 28-km depth (fig. 9), that is distributed across a 4-km-wide zone which coincides with, and extends eastward of, the deformation zone imaged in the upper crust. Together, these observations define a steeply dipping fault zone that extends from the near surface to the base of the crust.

The seismicity in the vicinity of the Kirby Hills Fault zone, as recorded by the USGS' Northern California Seismic Network (Calnet) since May 1974, is plotted in figure 9. South of lat 38°10′ N., the seismicity (cross secs. *A*–*A*′, *B*–*B*′, fig. 9) and focal mechanisms (fig. 10*A*) indicate that the fault dips from near vertical to 65° NW. North of this latitude (cross sec. *C*–*C*′, fig. 9), the seismicity and associated focal mechanisms indicate a complex pattern of strike-slip and reverse faulting (fig. 10*A*). Earthquakes are located within a layered velocity model developed by a joint hypocenter-velocity inversion specifically for this area. The 544 (out of a total of 621) earthquakes plotted have horizontal and vertical uncertainties of 2.5 and 5.0 km, respectively.

The deepest seismicity locates the Kirby Hills Fault at the base of the crust. These unusually deep earthquakes, which occur within a few kilometers of the Moho (for example, Holbrook and others, 1996) indicate that the fault is seismogenic throughout the crust. Such deep seismicity is highly unusual and suggests that the Kirby Hills Fault zone extends as a steeply dipping structure from the surface all the way to the base of the crust.

Representative focal mechanisms, determined from *P*-wave first-motion observations recorded by the Calnet, have also been analyzed (fig. 10*A*). All mechanisms have at least 40 first-motion observations. Motion is predominantly right-lateral strike slip on northwest-oriented faults, but thrust faulting also occurs on west-northwest-oriented planes north of the Sacramento River. The focal-mechanism studies are compatible with an 80°-E.-dipping fault plane (figs. 9, 10).

The earthquake activity near Pittsburg (figs. 1, 4) extends ~25 km northward and ~5 km southward of the Sacramento

River. To the north, the seismicity coincides with the mapped trace of the Kirby Hills Fault. To the south, it dies out near the north limit of the Kirker fault at the north edge of the Diablo Range. These results support the interpretation by Krug and others (1992), who proposed that the Kirby Hills and Kirker Faults are linked together in an ~65-km-long system of faults which they labeled the Kirby Hills Fault system. Thus, the Kirby Hills Fault system may be an important element in the ongoing crustal deformation in the eastern San Francisco Bay region.

Combining results from high-resolution seismic techniques with intermediate- and low-frequency sources, as well as with relocated earthquake hypocenters, allows us to image the entire Kirby Hills Fault zone through the crust (fig. 10*B*). The high resolution data reveal a 1.0-km-wide zone of 3°–5°-W.-dipping strata unconformably overlain by a 30- to 40-m-thick package of westward-thickening prograding sedimentary rocks. The localization of these dipping strata and the conspicuous angular unconformity that separates them suggest a recent episode of tilting and erosion. The deeper seismic-reflection profiles show this zone of deformation extending downward to at least 6-km depth, on the basis of a series of reflector offsets in the upper 2- to 3-s two-way traveltime. Seismicity is distributed across a 4-km-wide belt that

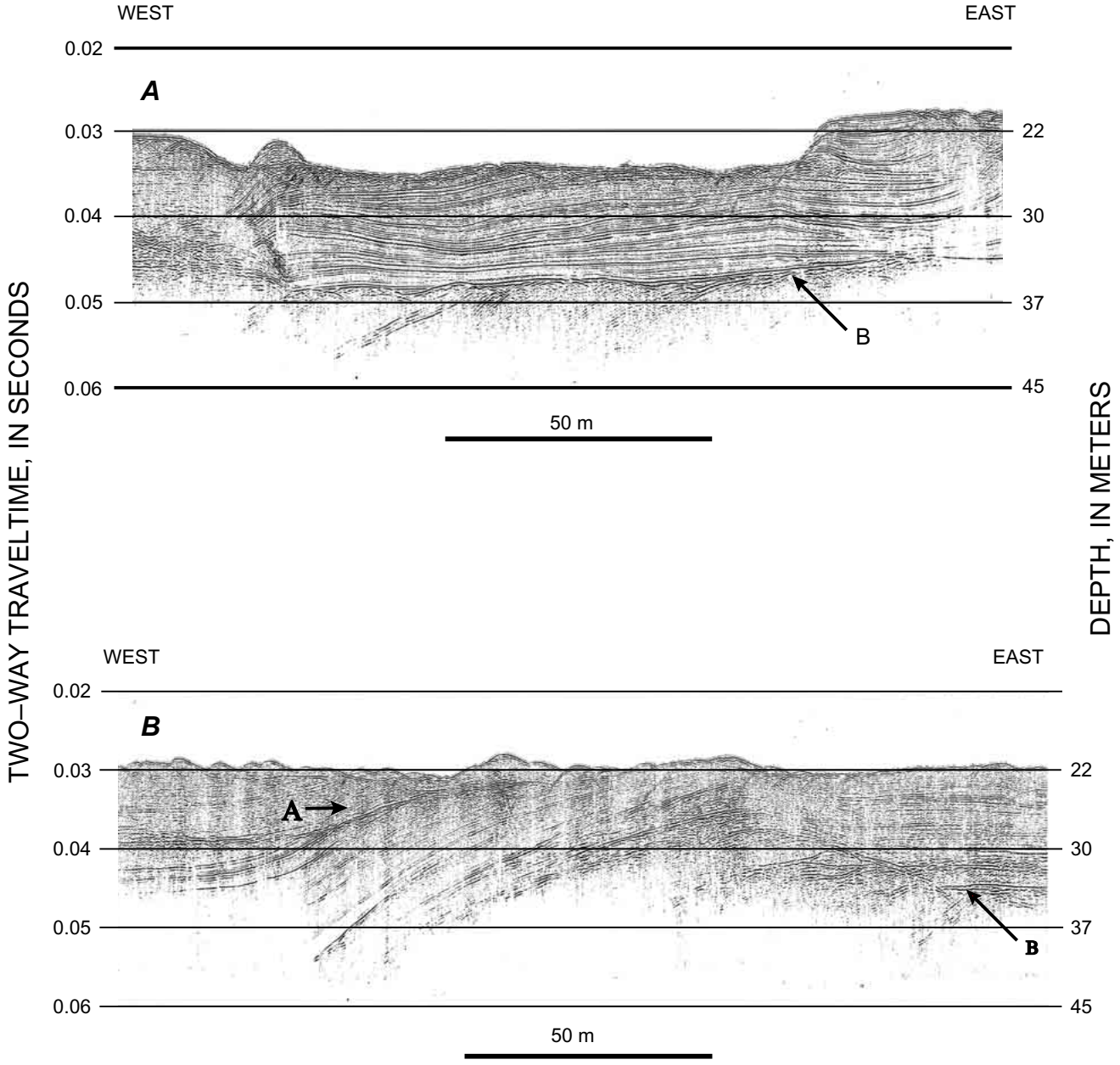

Figure 5.—Ultra-high-resolution seismic-reflection profiles gathered east (*A*) and west (*B*) of the Kirby Hills Fault zone (figs. 1, 4), showing significant deformation of youngest sedimentary rocks in fault zone. Approximately 200-m gap separates the two profiles, both of which fall within the 1-km-wide Kirby Hills Fault zone (fig. 4). Reflectors A and B are unconformities.

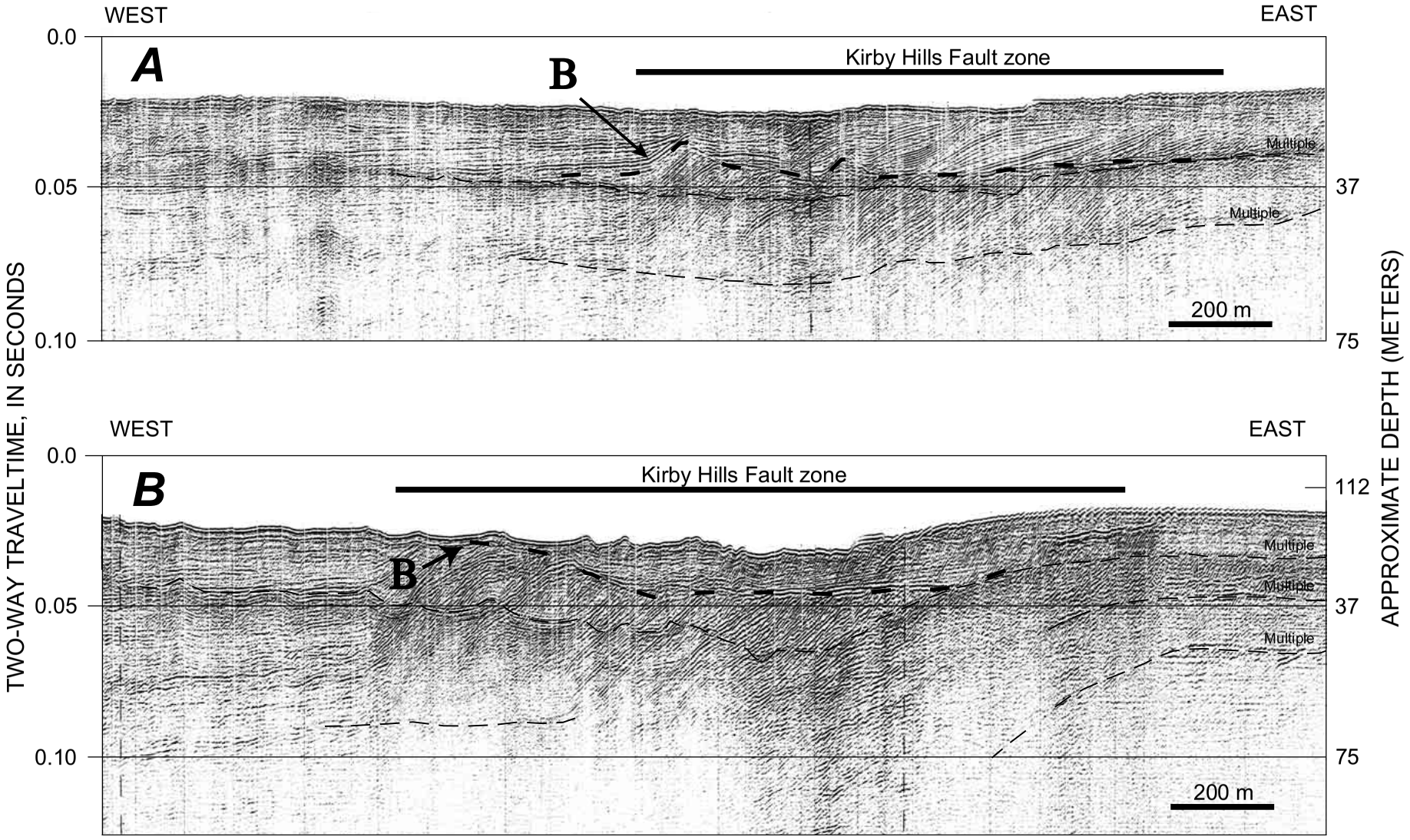

Figure 6.—High-resolution seismic-reflection profiles of the Kirby Hills Fault zone (figs. 1, 4), showing warping and deformation unconformity (reflector B, fig. 5). Relative locations of profiles are shown in figure 7 (boxes). Vertical exaggeration, X 7.5.

coincides with, and extends eastward of, the deformation zone imaged in the upper crust. Together, these observations define a near vertical or steeply (>75º–90º) east-dipping fault zone that extends from the near surface down almost to the base of the crust. Focal mechanisms indicate predominantly strike-slip faulting.

1995: Three-Dimensional Upper-Crustal Velocity Structure in the San Francisco Bay Region

A three-dimensional seismic-velocity model of the San Francisco Bay region provides useful information for seismic hazard analysis: (1) a detailed three-dimensional model is needed to better predict strong ground motion during an earthquake because the travelpaths of seismic waves are governed by the velocity structure; (2) a three-dimensional velocity model allows proper analysis of crustal fault-plane reflections, (3) earthquake hypocenters can be better located, and focal mechanisms can be more accurately determined; and (4) subsurface fault zones can be mapped where insufficient microseismicity exists to identify them directly. We thus conducted inversions for the regional velocity structure, using earthquake and controlled seismic sources. Calnet has been recording earthquakes in the San Francisco Bay region since the 1960s. Over time, a vast catalog of quality earthquake

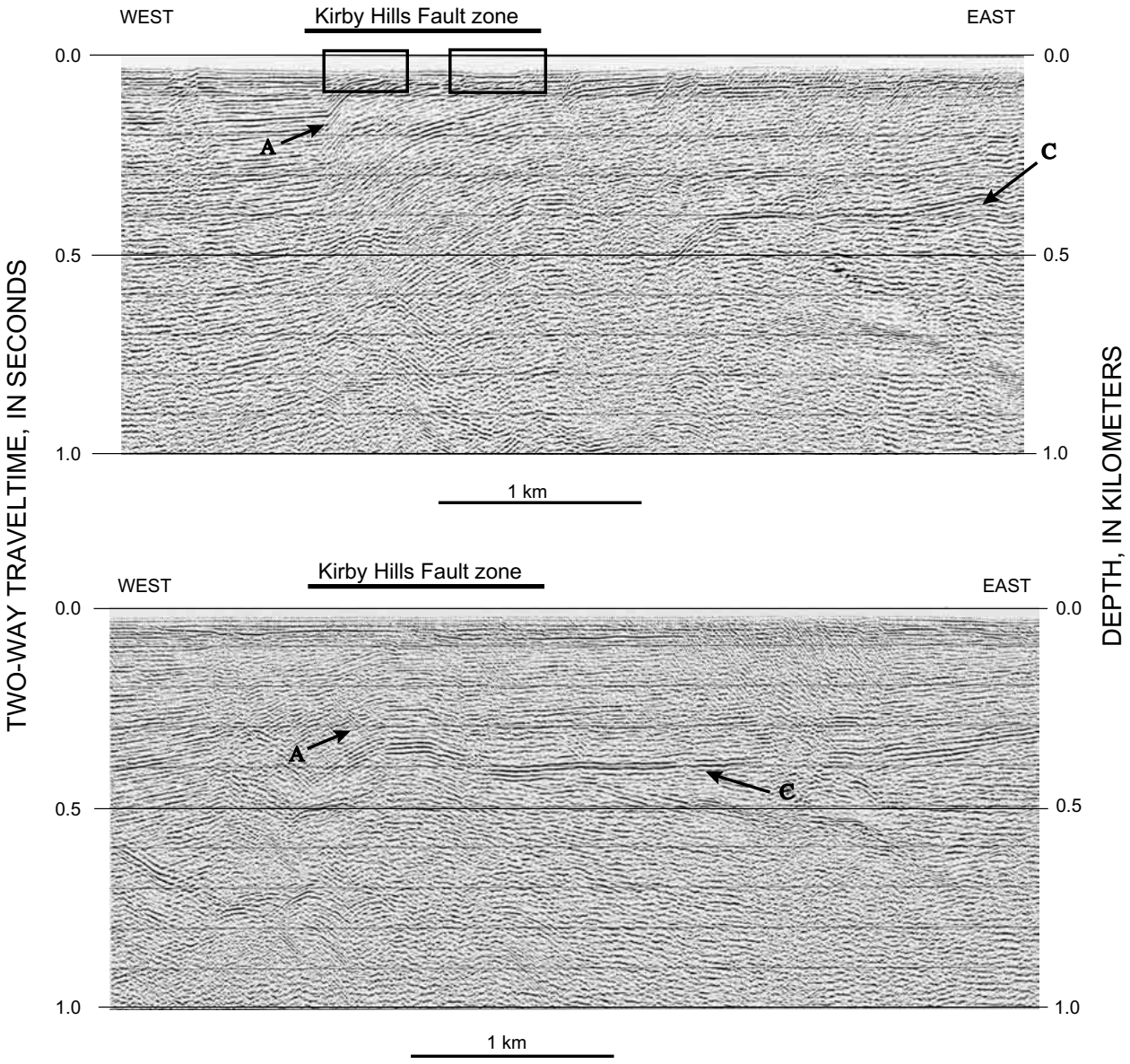

Figure 7.—Intermediate-resolution seismic-reflection profiles across the Kirby Hills Fault zone (figs. 1, 4), documenting an abrupt deformational front, east of which reflections are abruptly folded in an eastward-vergent geometry. Although this folding extends to at least 600-m depth, no fault-plane reflections are evident. Without clear images of fault plane, it is difficult to constrain style of faulting, whether fault-bend folding or fault-propagation folding. Boxes show locations of high-resolution profiles in figure 6.

arrival times has accumulated. We used this catalog in concert with the growing number of controlled sources recorded in and around San Francisco Bay to construct a three-dimensional model of the upper-crustal velocity structure of the bay region and, with the aid of a temporary local network, the detailed velocity structure of the northern part of the San Francisco peninsula.

Velocity-Modeling Methods and Data

We applied the three-dimensional tomographic technique of Hole (1992), modified to simultaneously invert for velocity, hypocenters, and origin times. This technique applies a finite-difference solution to the eikonal equation (Vidale, 1990; updated by Hole and Zelt, 1995) to calculate first-arrival times through a gridded slowness model. An iterative nonlinear inversion is performed as a simple back-projection along raypaths determined from the forward-modeling step.

We compiled traveltime picks from various sources for each receiver as a function of their three-dimensional source locations and inverted them for three-dimensional velocity structure. Four types of traveltime data were applied to our velocity modeling: (1) first-arrival times from local earthquakes on temporary networks, (2) first-arrival times from airgun blasts in San Francisco Bay, (3) first-arrival times from chemical-explosive sources detonated on land, and (4) traveltime picks from earthquake and controlled sources from the Calnet catalog and previous regional seismic experiments (Murphy and others, 1992; Brocher and Moses, 1993; McCarthy and Hart, 1993; Brocher and Pope, 1994; Kohler and Catchings, 1994; Holbrook and others, 1996).

Initial hypocenter locations and origin times of earthquakes were inputted as determined by Calnet. Starting models were discretized into grids of 1-km cells; we used small grid cells to ensure accurate calculation of raypaths along short source-receiver offsets. A spatial-smoothing filter was applied to the models between velocity and source-parameter iterations. Early iterations were conducted that tested various one-dimensional starting models with very broad smoothing filters (max 100 km), including only limited ranges of source-receiver offsets to solve the shallowest parts of the velocity model first. Subsequent iterations were conducted that included greater source-receiver offsets and progressively shorter smoothing filters.

The San Francisco Bay region is crossed by several major strike-slip faults that provided most of the seismicity we used to develop the velocity models presented here. These strike-slip faults also cause discontinuities in the velocity structure at seismogenic depths. The earthquakes used in this study were initially located with a one-dimensional veloc-

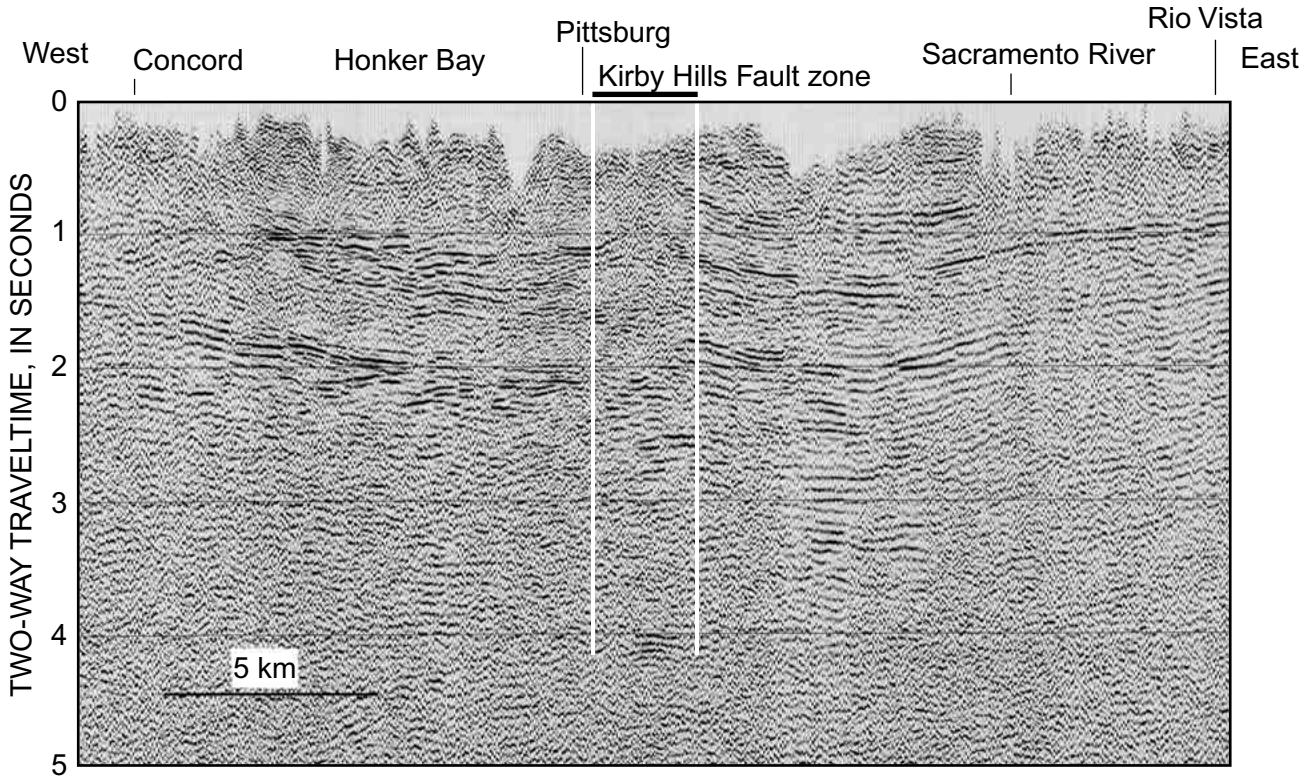

Figure 8.—Multichannel seismic-reflection profile across the Kirby Hills Fault zone (figs. 1, 4). Deformed rocks associated with fault zone are imaged from near surface to about 3-s two-way traveltime (~6–9-km depth). Heavy black line, Kirby Hills Fault zone as mapped by higher-resolution methods.

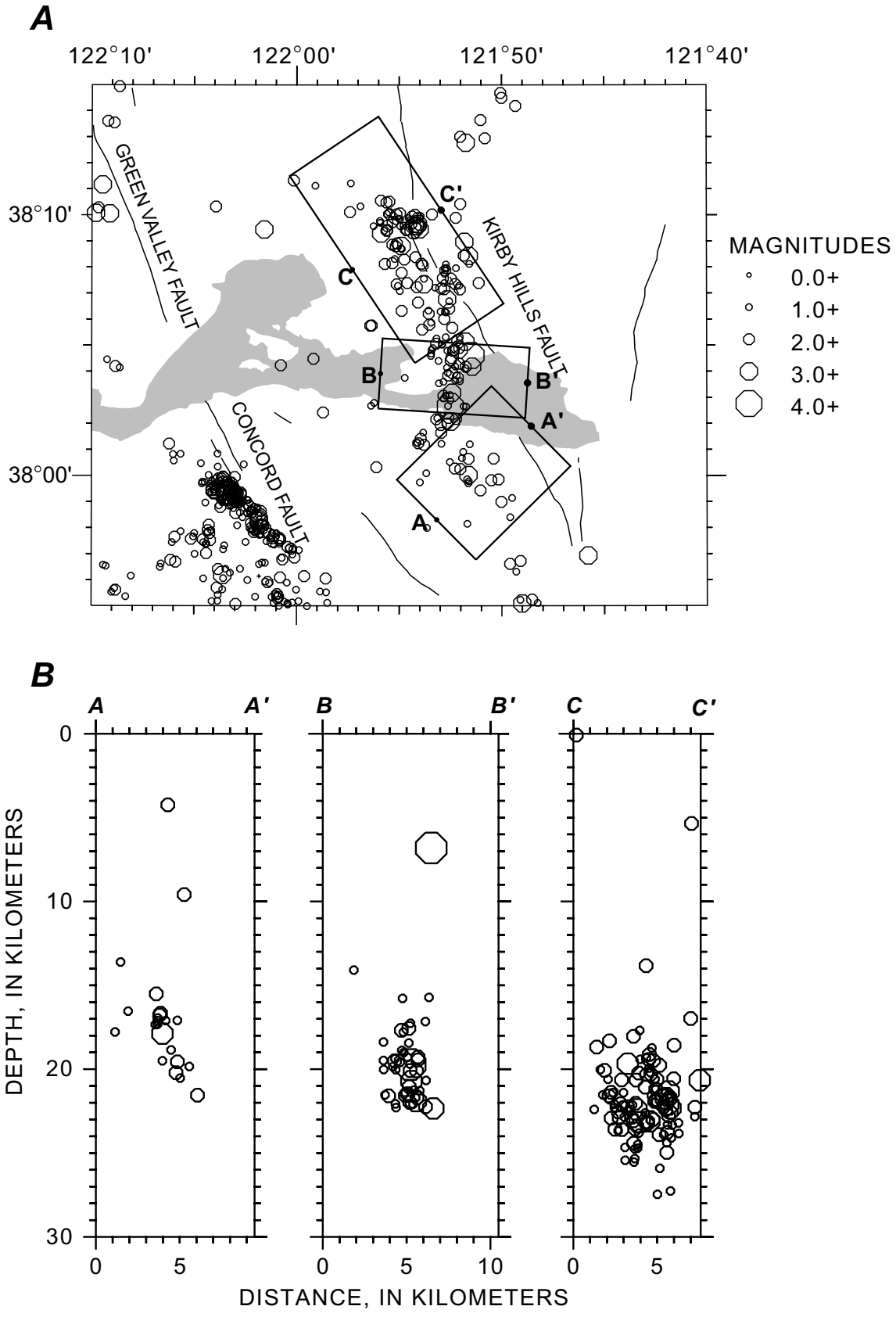

Figure 9.—Kirby Hills Fault zone (see figs. 1, 4 for location). *A*, linear trend of seismicity extending southward from where fault is mapped by marine investigations suggests that fault is ~50 km long. *B*, Depth cross sections of hypocenters, illustrating deep seismicity associated with the Kirby Hills Fault zone that extends to base of crust.

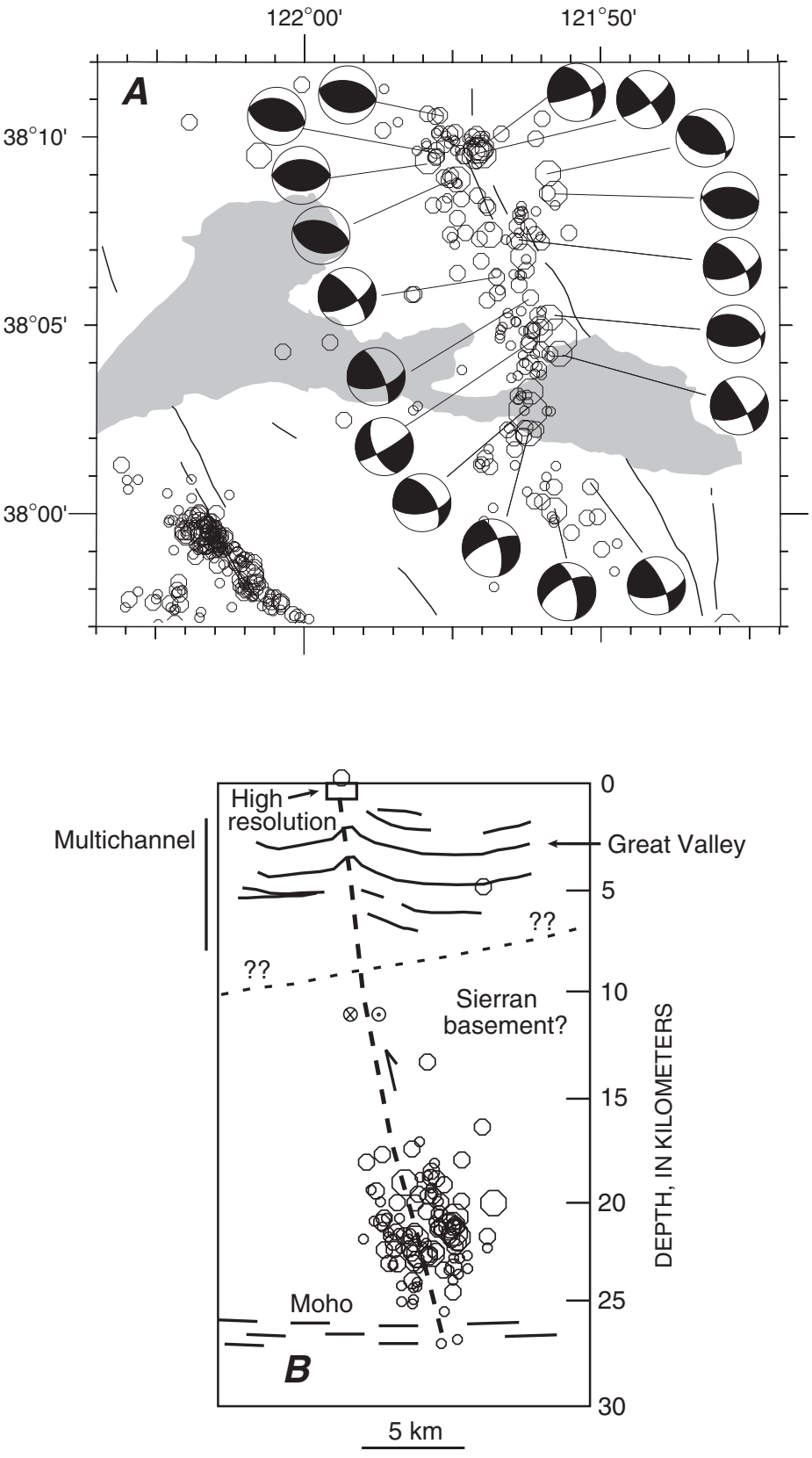

Figure 10.—Kirby Hills Fault zone (see figs. 1, 4 for location). *A*, Focal mechanisms of seismicity associated with zone. All mechanisms have at least 40 first-motion observations. Motion is predominantly right-lateral strike-slip on northwest-oriented faults, but thrust faulting also occurs on west-northwest-oriented planes north of the Sacramento River. *B*, Schematic interpretation of the Kirby Hills Fault zone based on various data constraints.

ity model; thus, a degree of coupling between hypocenter location and the velocity structure derived from earthquake traveltimes is unavoidable and could cause significant errors in the resolved velocity models (Thurber, 1993). To reduce such errors, hypocenters and origin times were relocated with controlled source locations and times held fixed. The events were relocated between velocity iterations (mean relocation, 0.54 km; see Hole, 1992, and Hole and others, 2000, for full details on the traveltime-inversion algorithm).

Regional Three-Dimensional Velocity Structure of the San Francisco Bay Region

Combined earthquake and controlled source traveltime data reveal a three-dimensional structural image of the seismogenic crust in the San Francisco Bay region from ~1–2-km down to ~18-km depth (Parsons and Zoback, 1997; Hole and others, 2000). The three-dimensional velocity structure was inverted from 234,270 traveltime picks resulting from 7,742 earthquake arrivals recorded at 160 stations, and 2,874 controlled source-receiver pairs. We present a geologic interpretation of the seismic-velocity model below.

The model shows generally higher velocity west of the Hayward Fault at most depths (fig. 11). The Calaveras, Hayward, and Rodgers Creek Faults together show the strongest and most consistent correlation between surface fault trace and apparently offset rock bodies at depth. South of the Sacramento River delta, the Hayward and Calaveras Faults mark the boundary between higher-velocity Franciscan and lower-velocity Great Valley rocks. That boundary persists at depth to the base of model coverage at about 18-km depth (fig. 11). The consistent, well-developed velocity contrast across the Hayward and Calaveras Faults relative to the San Andreas Fault may result from their relatively larger cumulative offset (50–70 km versus 19–23 km; Cummings, 1968; McLaughlin and others, 1996).

In the uppermost ~10 km of crust, high velocities are characteristic beneath San Francisco Bay between the Hayward and San Andreas Faults, which is interpreted as Franciscan basement (Hole and others, 2000). A local low-velocity anomaly beneath central San Francisco Bay (fig. 11) that correlates with the San Leandro Basin of Marlow and others (1999) seems to be no more than 4 km deep; another ~5-km-thick basin underlies the Santa Clara Valley. East of the Calaveras Fault, sedimentary rocks of the Great Valley cause a low-velocity anomaly that persists to at least 12-km depth.

Beneath ~8-km depth, a clear boundary emerges between higher-velocity Salinian rocks west of the San Andreas Fault and Franciscan rocks to the east (fig. 11). This boundary persists to at least the base of model coverage at 18-km depth and is especially pronounced north of the Loma Prieta rupture zone on the San Francisco peninsula. The Salinia-Franciscan terrane boundary is not apparent north of the Golden Gate.

North of the Sacramento River delta, high-velocity rocks appear to be offset east of the Rodgers Creek Fault (fig. 11). The surface geology is complex east of this fault, comprising slivers of the Franciscan terrane, Great Valley sequence, ultramafic rocks associated with the faulted terrane boundary, and Cenozoic volcanism. The seismic-station coverage is relatively sparse in this area, and the spatial resolution is larger than the geologic units, and so the model may be averaging the effects of shallow igneous rocks. Relatively high seismic velocity persists to at least 11-km depth beneath the Sonoma Volcanic Field but not beneath The Geysers and the Clear Lake Volcanic Field farther north, similar to the less well resolved deep results of Stanley and others (1998).

The primary features of the upper-crustal structure of the San Francisco Bay region revealed by the three-dimensional tomography model are the strong lateral velocity contrasts across major right-lateral strike-slip faults. These contrasts indicate that the faults are high angle down to at least ~15-km depth into the crust. The strong crossfault velocity contrasts affect calculations of earthquake focal mechanisms, hypocenter locations, and strong-ground-motion simulations because seismic energy can be refracted laterally along such velocity boundaries. These effects are not accounted for in traditional one-dimensional model calculations.

Detailed Three-Dimensional Velocity Structure of the San Francisco Peninsula

The geology of the San Francisco Peninsula is dominated by the right-lateral San Andreas Fault. In most of central California, the San Andreas Fault bounds the Salinia and Franciscan terranes. On the San Francisco peninsula, however, the Salinia-Franciscan terrane boundary is marked by the subparallel Pilarcitos Fault west of the San Andreas Fault (figs. 3, 11; see Brabb and Pampeyan, 1983). On the surface, the San Andreas Fault on the San Francisco peninsula is contained entirely within the Franciscan Complex. At least two possible models for the arrangement of the Salinia-Franciscan terranes on the peninsula have been proposed: (1) the Pilarcitos Fault may be an east-dipping thrust fault that has emplaced Franciscan rocks over Salinian granites (fig. 12; see Wakabayashi and Moores, 1988), or (2) the Pilarcitos Fault may represent an old segment of the San Andreas Fault system that accommodated pre-Quaternary right-lateral slip, and so it is a high-angle structure (fig. 12; see Cummings, 1968; McLaughlin and others, 1996). The surface trace of the Pilarcitos Fault has a somewhat curved or scalloped appearance that makes it look more like a thrust fault than a strike-slip fault, and the fault trace is associated with east-dipping mylonite fabrics indicative of shortening (Wakabayashi and Moores, 1988). However, the relation, if any, between the mylonite and the Pilarcitos Fault remains unresolved.

A temporary seismograph network was deployed on the San Francisco peninsula during the first half of 1995 to use local earthquake and controlled-source traveltimes to create a detailed upper-crustal structural model of the San Andreas and associated faults. The goal of this study was to determine which of the two possible models for the arrangement of

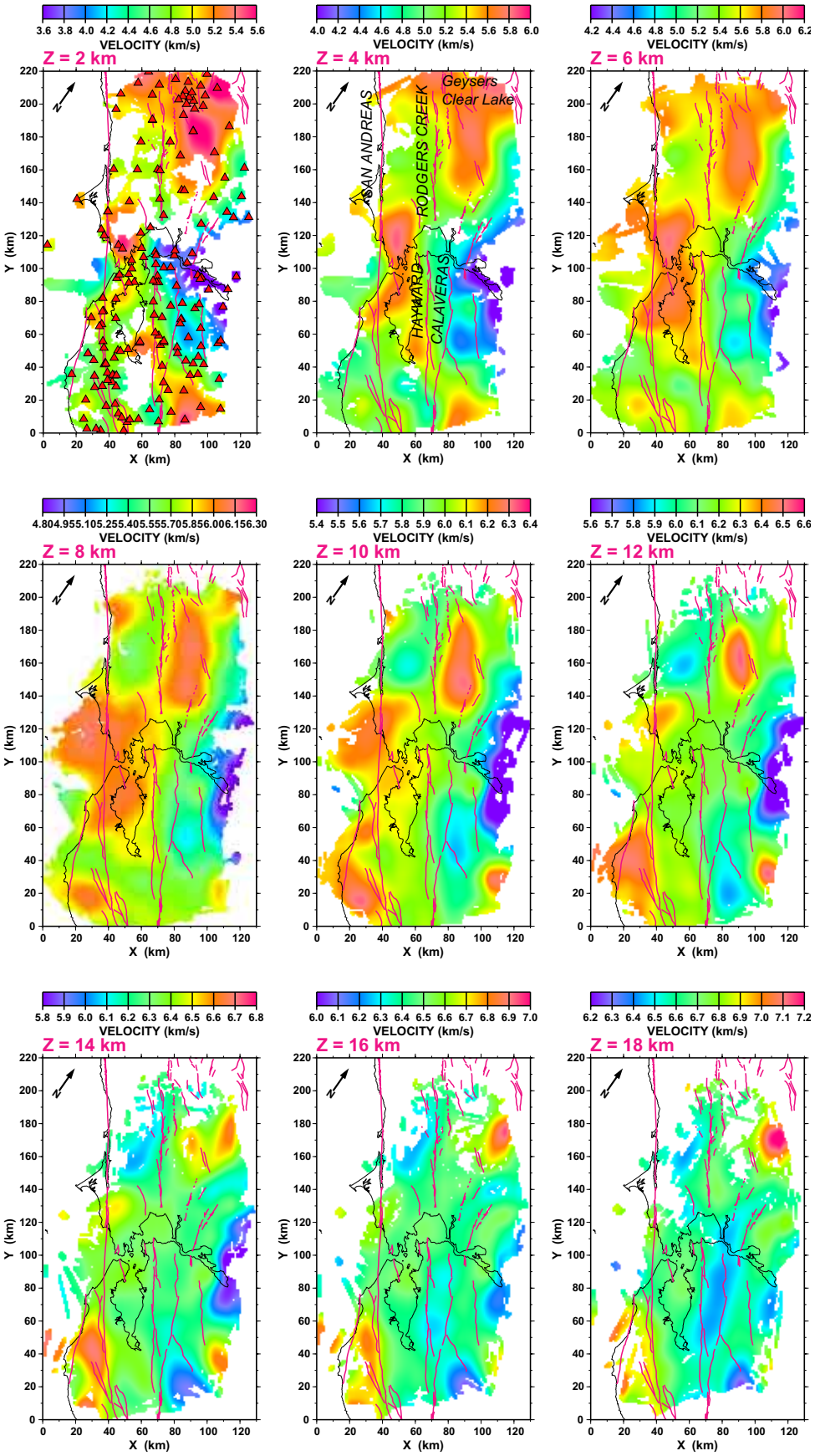

Figure 11.—Horizontal slices from a three-dimensional velocity model of the San Francisco Bay region taken at 2-km depth intervals. Colors represent variations in seismic velocity.

the Salinia-Franciscan terranes on the peninsula is correct. The answer to this question is important because an active Pilarcitos thrust fault could imply far more hazard to nearby San Francisco and peninsula cities than an extinct proto-San Andreas segment.

To make the best use of the San Francisco peninsula array, the regional velocity model was used to calculate traveltimes from earthquake sources located outside of the network to the edges of a second, more detailed model. Our 1- to 3-km-spaced network allowed for a much shorter smoothing filter than did the 5- to 20-km-spaced Calnet. Thus, in effect, the distant earthquake sources were migrated to the edges of a more detailed model and treated like deep sources along the model faces; this technique somewhat resembles a teleseismic experiment, in that traveltime variations from distant sources were used to augment a local-array study. The uncertainties in source location and traveltime misfits of the regional velocity model may accumulate on long travelpaths and could cause errors in the traveltime calculations to the edges of the more detailed model. In practice, however, such uncertainties manifested primarily as small static-velocity shifts at depth in the resolution tests. The application of controlled sources from known locations acted to calibrate the velocity models. In combination with fixed sources, short (2 km) smoothing parameters and the close (1–3 km) station spacing prevented significant spatial shifting of velocity anomalies. Intentional static mislocation of earthquake sources in test models caused only minor changes in resolved velocity.

A three-dimensional velocity model limited to the San Francisco peninsula was constructed by shortening the final smoothing filter to 2 km, in accordance with the 1- to 3-km station spacing adopted for the temporary seismic network. The San Francisco peninsula model converged to an root-mean-square traveltime misfit of 245 ms after five iterations. Horizontal slices (20 by 20 km) from the three-dimensional model volume are shown in figure 12. At 3 km depth, the highest-velocity (5.5 km/s) rocks appear to be confined between the downward vertical projection of surface traces of the San Andreas and Pilarcitos Faults and probably represent either a deeper expression of the Franciscan greenstone mapped at the surface, or a higher velocity unit underlying the Permanente terrane. Southwest of the Pilarcitos Fault, velocities are consistent with the large outcrop of Cretaceous granite (Montara Mountain Granite) that is part of the Salinian block (Brabb and Pampeyan, 1983).

Below 3- to 5-km depth, a downward vertical projection of the surface trace of the Pilarcitos Fault appears to mark a velocity transition from lower velocities (5.5–6.0 km/s) to the southwest into higher velocities (6.2–6.8 km/s) to the northeast (especially evident at 7-km depth, fig. 12). Our resolution tests indicate that below 6-km depth, velocity anomalies are resolvable only within ~2 km of their true positions. Thus, this lateral velocity change could reasonably be attributed to either the San Andreas or Pilarcitos Fault. Below 7-km depth are hints of structures that could be bounded by downward vertical projections of the Pilarcitos and San Andreas Faults, but coverage at these depths is limited, and such correlations are only tentative. More typical Franciscan velocities of ~6.0 to 6.2 km/s are observed at these depths.

An implication of the three-dimensional velocity model for the San Francisco peninsula is that at 3-km depth, possibly extending to 7-km depth, are velocity boundaries which are correlatable to the downward vertical projection of the Pilarcitos Fault (fig. 12). Such a correlation suggests that the Pilarcitos Fault may be a high-angle feature. High-angle velocity changes are also evident across the San Andreas Fault and are strongest in the shallowest part of the upper crust (1–3-km depth), where an apparent high angle boundary exists between the Franciscan Permanente terrane southwest of the fault and highly sheared Franciscan rocks to the northeast (fig. 12).

We conducted a higher-resolution two-dimensional traveltime inversion for the velocity of the Permanente terrane (bounded along its southwest side by the Pilarcitos Fault), using traveltimes recorded on instruments (SGRs) along a closely spaced (50-m station spacing, 2–3-km shot spacing) southwest-northeast-directed recording spread (fig. 3). The spread was oriented at an angle of ~90º to the strikes of the Pilarcitos and San Andreas Faults. Because of the short station spacing and overlapping coverage, we were able to reduce the velocity-model cell size to 100-m squares (in contrast to the 1-km cubes in the three-dimensional velocity models). Models derived from the two-dimensional higher-resolution seismic refraction data are most consistent with the Pilarcitos Fault as marking a vertical boundary in the uppermost 0.5 to 1.0 km of crust between relatively low velocity rocks of the Permanente terrane to the northeast (~4.5 km/s) and adjacent rocks of the Salinia terrane to the southwest (fig. 12*D*). The higher-resolution results tend to verify the indications from horizontal slices out of the three-dimensional velocity model that the Pilarcitos Fault is a steeply dipping boundary. We thus interpret the Pilarcitos Fault as primarily a strike-slip fault rather than a thrust fault. Before ~3 Ma, the Pilarcitos Fault probably accommodated most of the plate-boundary strain; a change in relative Pacific-North American Plate motions at ~3.9–3.4 Ma stimulated the formation of the Peninsular segment of the San Andreas Fault, and the Pilarcitos Fault was abandoned as the primary plate-boundary fault (Parsons and Zoback, 1997).

1995–97: Deep Configuration of the San Andreas and Hayward Faults from Crustal Reflections

After a few faint reflections were observed in the original BASIX data in 1991, the presence of deep crustal reflectors was firmly established by land and marine experiments in 1995 and 1997. BASIX–2 in April 1995 showed high-amplitude reflections between 6- and 10-s two-way traveltime. In June 1995, land-based explosive sources were added that generated high-amplitude reflections similar in appearance but at 11- to 13-s two-way traveltime. The disparity in arrival time with source-receiver position and strong reflection dip,

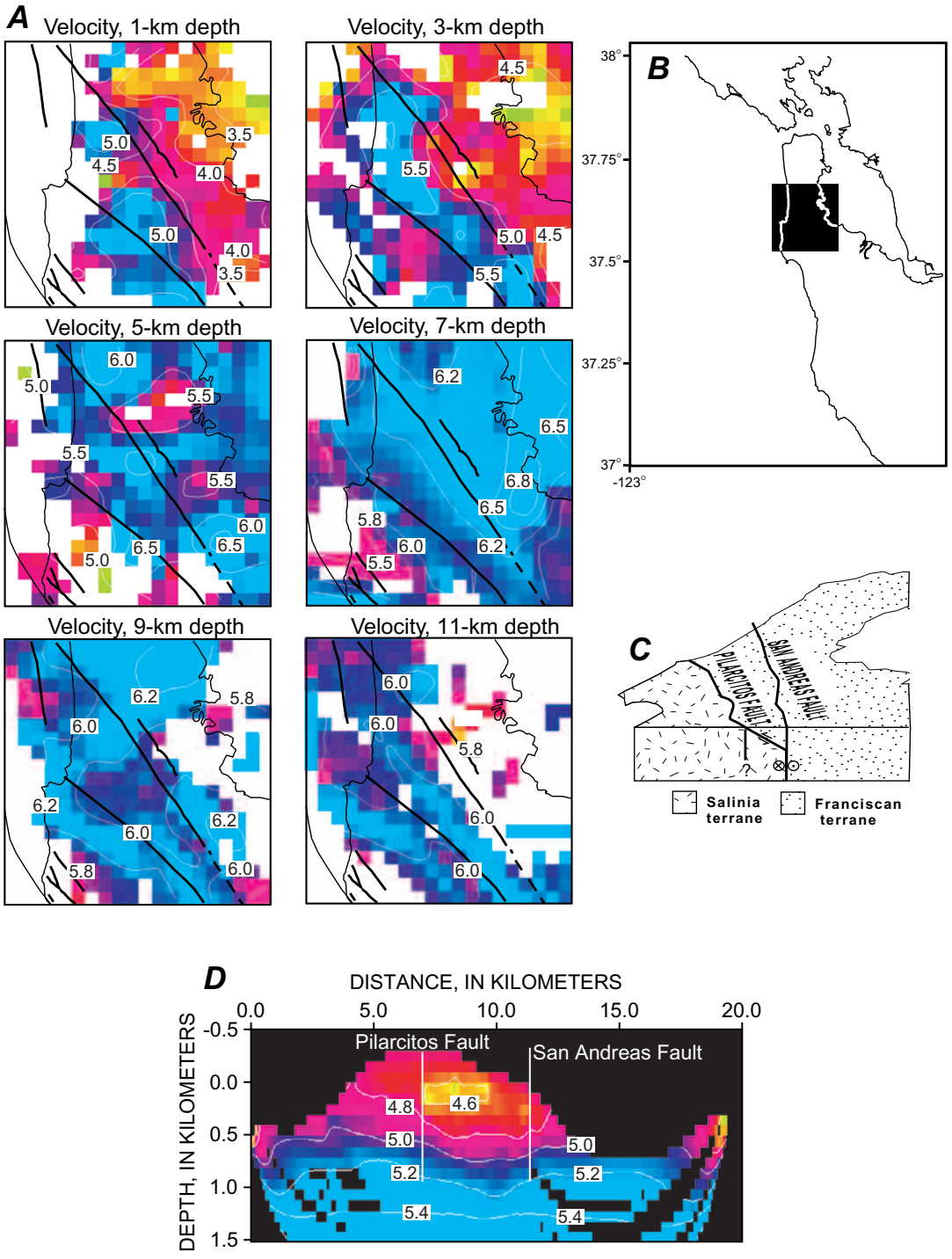

Figure 12.—San Francisco peninsula. *A*, Horizontal slices from the three-dimensional velocity model from 1- to 11-km depth. Each slice represents a 20- by 20-km area. Color scale for velocity differs from slice to slice to highlight velocity variations. Velocity contours in kilometers per second. Black lines, downward vertical projections of surface traces of the Pilarcitos and San Andreas Faults and coastlines. *B*, Sketch map of the San Francisco Bay region, showing boundaries of horizontal slices shown in figure 12A. *C*, Simplified geology of the San Francisco peninsula, showing possible structural models for relation between the Pilarcitos and San Andreas Faults. In most of central California, the San Andreas Fault separates the Salinia and Franciscan terranes, whereas on the San Francisco peninsula the Pilarcitos Fault marks the terrane boundary. The Pilarcitos Fault may be either an east-dipping thrust fault that has pushed Franciscan rocks up over Salinian rocks, or a vertical strike-slip fault that accommodated significant right-lateral slip before formation of the San Andreas Fault on the San Francisco peninsula at ~3 Ma. *D*, High-resolution velocity cross section (inverted from explosive sources) across the San Andreas and Pilarcitos Faults, showing high-angle velocity contrasts associated with the two faults.

or moveout (the change in reflection traveltime as a function of source-receiver offset), inspired a third marine experiment (BASIX–3) in 1997. Collectively, these seismic-reflection data enabled us to model the deep structure related to the Hayward and San Andreas Faults.

Crustal Characteristics from Vertical-Incidence Reflection Data

Large-airgun and chemical sources deployed in and around San Francisco Bay returned reflection energy throughout the crust (for example, Brocher and others, 1994; Parsons, 1998; Parsons and Hart, 1999), enabling some discussion on background reflectivity. The land-receiver spread crossed the Salinia terrane southwest of the Pilarcitos Fault and the Franciscan Complex between the Pilarcitos and San Andreas Faults on the San Francisco peninsula, and the marine receivers were all located within the Franciscan Complex (figs. 3, 12). These bedrock units show no coherent reflections down to about 5- to 6-s two-way traveltime (~14–15-km depth) over the entire source bandwidth (2–40 Hz; fig. 13).

Below about 5- to 6-s two-way traveltime, the land data best show an onset of discontinuous midcrustal and lower-crustal reflectivity (individual crustal-reflection segments generally less than 1 km long) that extends to the inferred Moho (~8–9-s two-way traveltime, 24–28-km depth). This depth to the Moho agrees reasonably well with models from wide-angle seismic data (Catchings and Kohler, 1996; Holbrook and others, 1996) that found Moho depths of 22 to 26 km beneath the Golden Gate and near San Francisco Bay. The seismic-reflection data do not show a discrete Moho reflection but rather a progressive decrease of reflectivity that can be traced most clearly on the amplitude-decay curve (fig. 13). The background midcrustal reflections are far less evident in the marine data because they tend to be suppressed by more nearly continuous, higher-amplitude dipping reflections.

The onset of midcrustal and lower-crustal reflectivity at 5- to 6-s two-way traveltime corresponds to a step in crustal velocity (6.4–7.3 km/s) at ~20-km depth, as modeled by Holbrook and others (1996). Because of wide observation in the San Francisco Bay region of an onset of reflectivity and associated change in crustal velocity at ~20 km depth, and the choppiness and discontinuity of the reflections, we interpret the lower-crustal reflectivity beneath the San Francisco peninsula as resulting from an increase in shear fabric, possibly due to a rheologic change at ~20-km depth (for example, Holbrook and others, 1996). Lower-crustal reflectivity, which is generally observed in terranes that have been transported long distances along strike-slip faults, such as beneath the central California margin and in Alaska, has been attributed to lower-crustal shearing during translation (Beaudoin, 1994).

High-Amplitude Dipping Reflectors

The most distinctive feature of vertical-incidence seismic records from the San Francisco Bay region (fig. 14) is late-arriving (6–13-s two-way traveltime) reflections with high amplitude, strong continuity, large moveout, and variations in traveltime and moveout with source-receiver position (figs. 13–16). If these events had been reflected from a single, flat horizon, very little change in traveltime or moveout would be expected. Reflections from a flat surface have predictable dip and obey the normal moveout equation

$$t = \frac{x_2^2 - x_1^2}{2V^2 t_0},$$

where t is the time, x_1 and x_2 are the reciprocal source and receiver positions, V is the seismic velocity, and t_0 is the zero-offset reflection time. Significant departure from normal moveout implies a reflection from a dipping interface; variation in moveout with source-receiver orientation can indicate the strike and dip of the reflector. Most of the high-amplitude reflections observed at vertical incidence must be distinguished from those regionally observed at wide source-receiver aperture from a near-horizontal reflector interpreted as the top of mafic lower crust by Brocher and others (1994) and Holbrook and others (1996).

High-Amplitude Dipping Reflections Recorded on Land

Following Moho traveltimes (~9-s two-way traveltime), a band of continuous (max 5 km long), high-amplitude reflections appears at ~11- to 13-s two-way traveltime on a land transect across the San Francisco peninsula (figs. 3, 13). The relative amplitude of these reflections is surprisingly high (5 dB above background; fig. 13). For reference, the relative amplitudes reported for the Death Valley, Socorro, and Surrency brightspots range from 8.5 to 10 dB; the Death Valley and Socorro brightspots were interpreted as magma bodies (Brown and others, 1987). A consistent directivity is evident in the events at 11- to 13-s two-way traveltime; they all dip southwest and are reflected from a horizon that must be located northeast of all the shots and the recording spread (fig. 3). These events cannot be explained by *P*-wave Moho reflections because the long traveltimes at crustal velocities would imply at least a 40-km-thick crust beneath San Francisco Bay, inconsistent with interpretations of wide-angle seismic data (Page and Brocher, 1993; Catchings and Kohler, 1996; Holbrook and others, 1996), regional elevations, or the Bouguer gravity anomaly. Such origins for these events as crustal *S*-wave or upper-mantle *P*-wave reflections were ruled out by Parsons (1998).

Marine High-Amplitude Dipping Reflections

High-amplitude dipping reflections were observed from many consecutive airgun blasts at 6- to 9-s two-way traveltime throughout San Francisco Bay (figs. 15, 16). These events are nearly identical to the reflections at 11- to 13-s two-way traveltime recorded on the San Francisco peninsula, except that most of the events at 6 to 9 s have earlier traveltimes. The reflections were recorded during all three

marine experiments in San Francisco Bay (BASIX–1 in 1991, BASIX–2 in 1995, and BASIX–3 in 1997), although in 1991 poor signal-to-noise conditions made interpretation difficult.

Strong reflections were observed in the pilot BASIX–2 in April 1995 when bottom cables were tested. Only three cable deployments were carried out in 1995 (fig. 14); all were oriented northwest-southeast, parallel to the dredged shipping channel in San Francisco Bay (see Hart and others, this volume, for detailed discussion). This orientation also proved to be nearly parallel to the strike of the dipping interfaces that produced strong reflections. As a result, most of the high-amplitude reflectors appeared to be relatively horizontal, although small excursions by the source or receivers from strike-parallel orientations caused unusually large reflection-moveout perturbations. These observations, tied to the similar, but much delayed, high-amplitude reflections recorded on land in June 1995, led us to question whether the events might be reflected from out-of-plane sources. We thus conducted BASIX–3 in 1997 to gather more data from different source-receiver orientations in order to measure the potential dip on the reflectors.

During BASIX–3 in 1997, we deployed bottom cables in a crossing pattern in the same area where high-amplitude reflections were recorded in 1995 (fig. 14), and made four more deployments oriented mostly southwest-northeast to augment the northwest-southeast-oriented cables deployed in 1995. Strong reflections were again observed after ~6-s two-way traveltime, but traveltime and moveout varied more widely than in the 1995 data.

Combined Traveltime Observations: Why the Reflections Cannot Come from a Horizontal Detachment Fault

Comparing the results from the 1995 land and marine experiments with the 1997 data, we find a consistent pattern of increased reflection moveout for source-receiver geom-

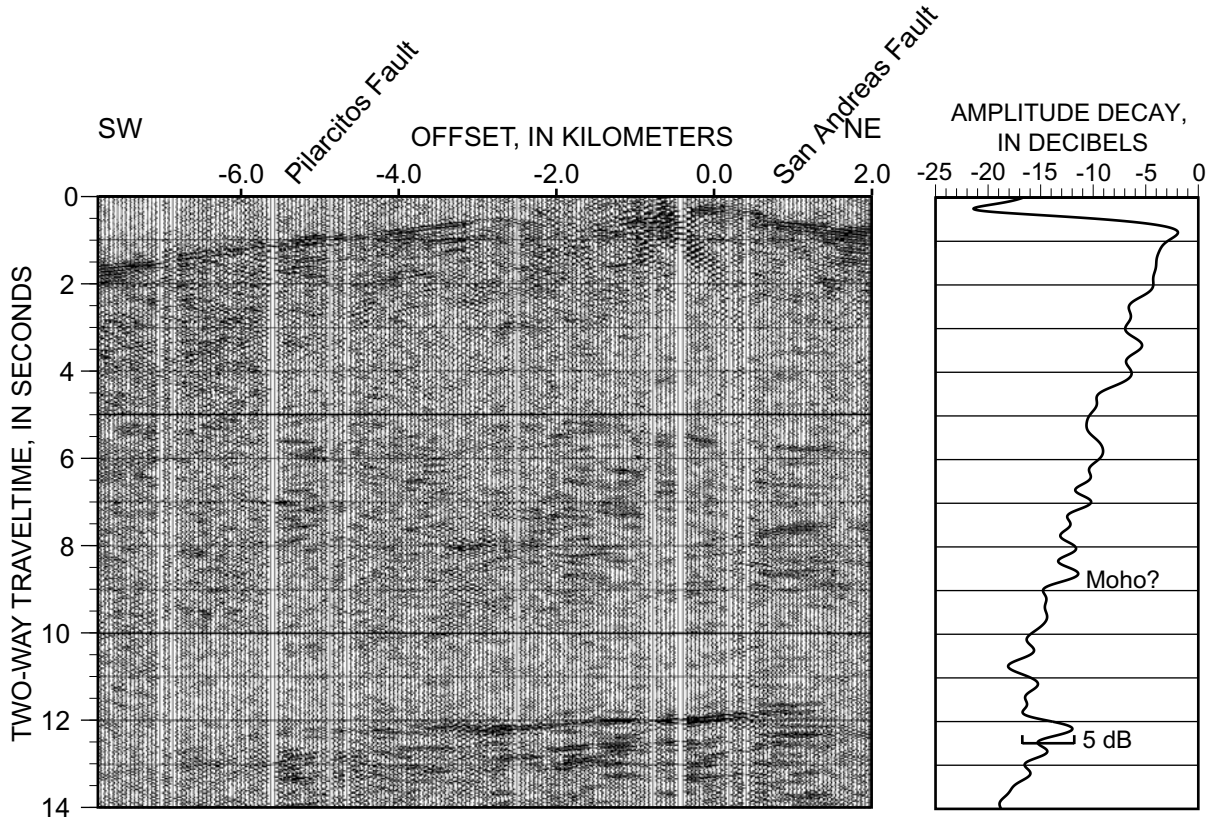

Figure 13.—Representative shot gather from an explosive source recorded by 183 Seismic Group Recorders. Shot was located at the San Andreas Fault on the San Francisco peninsula (see fig. 3 for location). Section shows a relatively transparent upper crust (no coherent reflections) in both the Salinia and Franciscan terranes. An onset of discontinuous midcrustal and lower-crustal reflectivity occurs at about 5- to 6-s two-way traveltime. No obvious changes in reflectivity are apparent across the San Andreas and Pilarcitos Faults on any shot gather. The Moho does not generate distinct reflections and is identified by a decrease in reflectivity at ~9 s two-way travel-time (visible on amplitude-decay curve). Beneath the Moho, shot gathers show southwest-dipping, high-amplitude reflections (5 dB above background) at ~11- to 13-s two-way traveltime. Amplitude-decay curve was calculated from 30 traces of gather stacked after normal-moveout and spherical-divergence corrections.

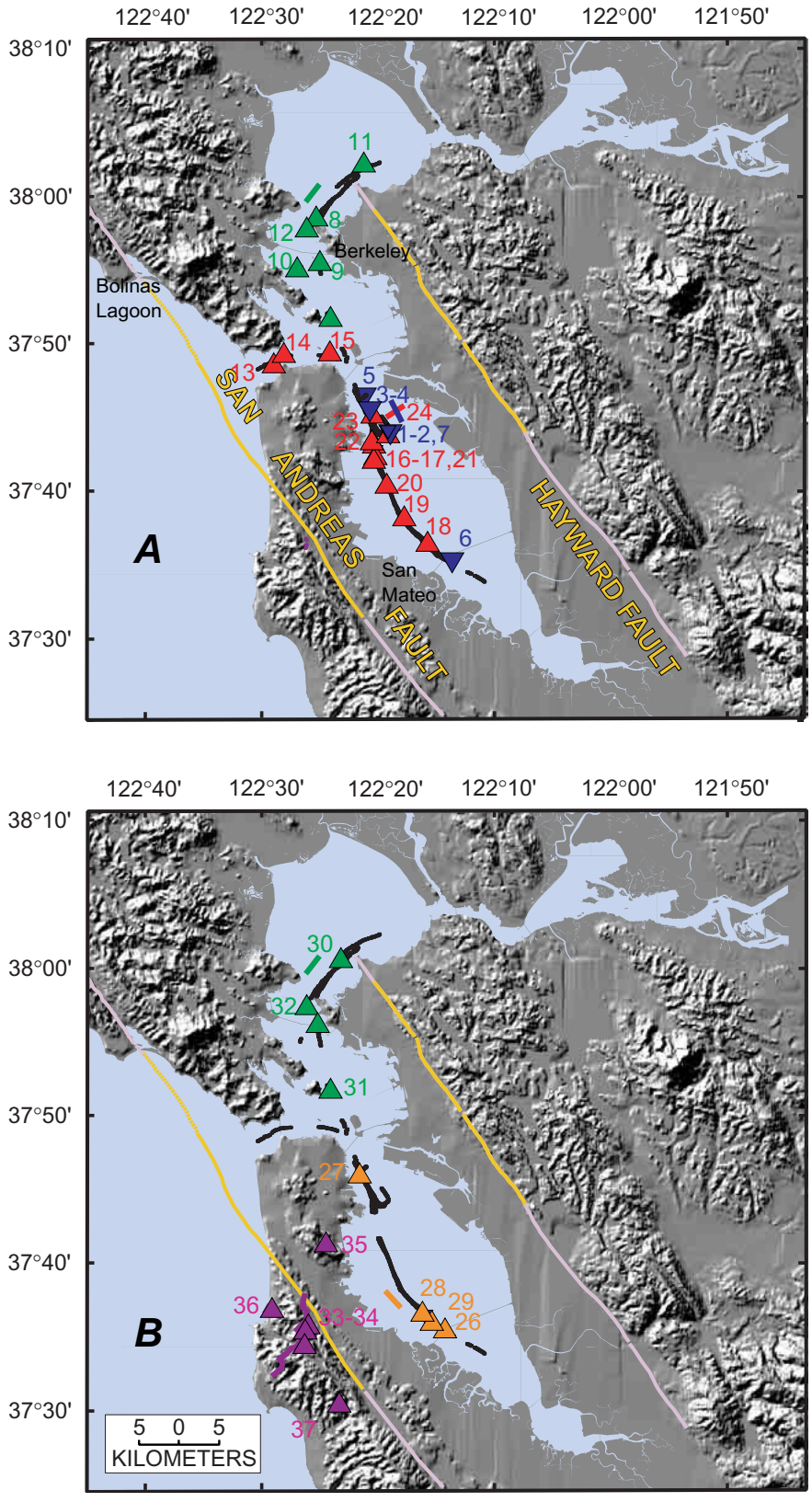

Figure 14.—San Francisco Bay region, showing locations of modeled arrivals from the San Andreas reflector (*A*) and Hayward reflector (*B*). Numbers correlate to gathers shown in figures 15 and 16. Colored triangles, source positions as recorded by bottom cables, represented by lines of same color.

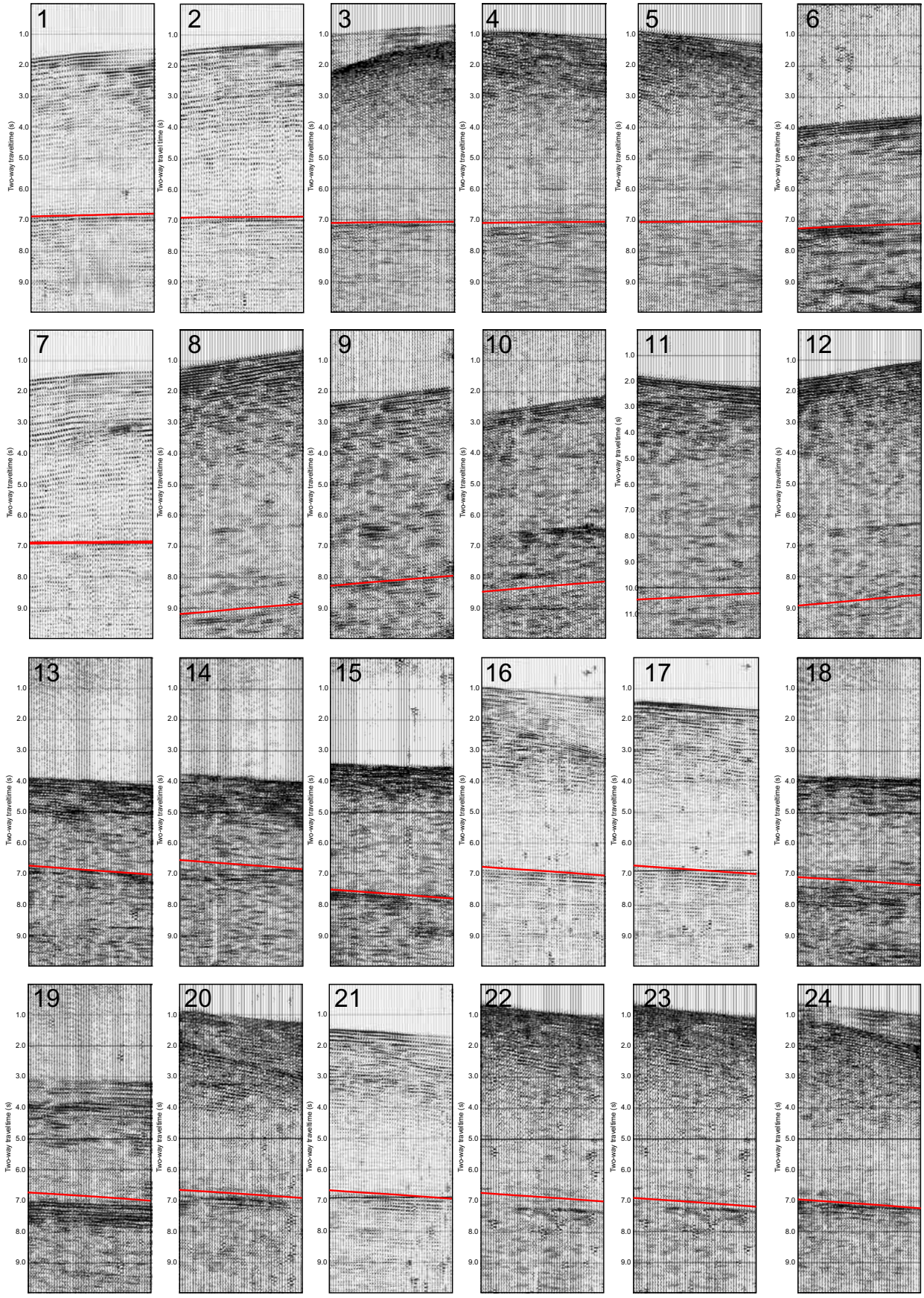

Figure 15.—High-amplitude reflections observed from different points throughout San Francisco Bay (fig. 14) and modeled traveltimes from San Andreas reflector (red lines). All gathers show 2.4 km of data. Offsets are mapped in figure 14.

etries oriented southwest-northeast relative to a northwest-southeast orientation. In addition, northeast-dipping events have progressively later traveltimes for source positions located farther eastward. Similarly, we observe a pattern of later traveltimes for southwest-dipping reflections with increasingly westerly source positions. These observations indicate that the regionally observed high-amplitude reflections at near-vertical incidence must be returning from at least two dipping interfaces deep in the crust or upper mantle which strike approximately northwest-southeast.

We recorded airgun sources on a crossing array of bottom cables in San Francisco Bay where high-amplitude reflections were known to occur. We observe a wide variation in reflection moveout as a function of bottom-cable azimuth. The expected normal moveout across a 2.4-km-long recording cable from a horizontal reflector at 7-s two-way traveltime

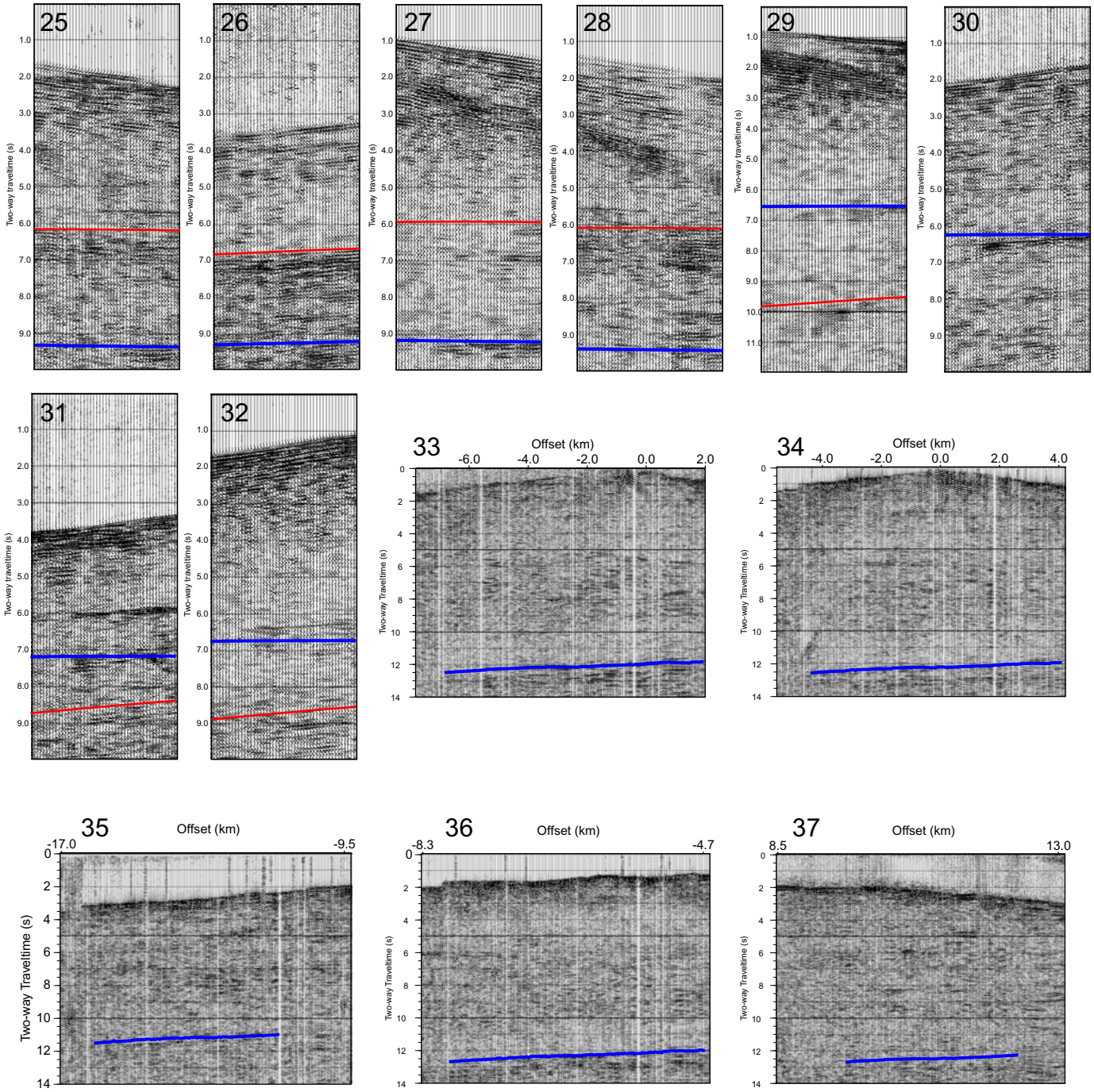

Figure 16.—High-amplitude reflections observed from different points throughout San Francisco Bay and peninsula (fig. 14), and modeled traveltimes from San Andreas (red lines) and Hayward (blue lines) reflectors.

for a shot positioned 2.5 km away from the cable is about 40 ms. Much larger moveout values (hundreds of milliseconds) imply a dipping reflector. Reflections recorded parallel to the San Andreas Fault are nearly horizontal at ~7-s two-way traveltime (fig. 17*A*), whereas reflections recorded orthogonal to the fault dip down to the northeast (more than 200-ms difference in moveout over a 2.4-km distance relative to the reflections recorded parallel to the fault; fig. 17*B*). If the reflector were horizontal, moveout would be independent of azimuth; thus, the reflector must dip down to the northeast. We note a consistent pattern of azimuthal dependence of moveout throughout San Francisco Bay (fig. 17*C*).

A dipping reflector causes offset dependence on reflection traveltime; if the source position is moved farther downdip from a fixed receiver, then the reflection traveltime is expected to be later. For example, in figure 18, the traveltime of the same reflection event progressively increases with shot distance from the San Andreas Fault. Such a relation can be explained only by a reflector with a steep downward dip to the northeast, somewhere in the vicinity of the San Andreas Fault. We observe a dependence of reflection traveltime (southwest-dipping events) on distance from the San Andreas Fault throughout the bay (fig. 18). We observe a second group of reflections with northeastward dip that have progressively later traveltimes with increasing source distance from the Hayward Fault; these events range in traveltime from ~6 s in San Pablo Bay to nearly 13 s recorded on the San Francisco peninsula (fig. 18).

These observations demonstrate that a model with near-horizontal reflectors beneath San Francisco Bay is inappropriate for the high-amplitude reflections. Therefore, a two-dimensional modeling approach that projects seismic raypaths into one vertical plane is also inappropriate. The combined geometry of the 1995 and 1997 land and marine seismic-reflection experiments is complex, and poorly suited for projection into one plane, even if the subsurface geology were simpler. Thus, any analysis of reflection traveltimes in the San Francisco Bay region must be treated as a three-dimensional problem.

Three-Dimensional Traveltime Modeling of High-Amplitude Reflections

We use three-dimensional finite-difference traveltime calculations (Hole and Zelt, 1995) to model the surfaces responsible for high-amplitude reflections recorded in San Francisco Bay (Parsons and Hart, 1999). We apply a three-dimensional velocity model for the region, constructed from earthquake sources (Parsons and Zoback, 1997; Hole and others, 2000) in combination with an extrapolation of a two-dimensional lower-crustal velocity model (Holbrook and others, 1996). The reflector that best satisfies all the northeast-dipping reflection traveltimes dips 60º beginning at 12-km depth and parallels the strike of the San Andreas Fault in the study area (fig. 19). The modeled reflector dip begins beneath the downward vertical projection from the surface trace of the San Andreas Fault (fig. 19). The uniqueness of this model is tested by a wide variety of shot-receiver offsets and reflection angles (figs. 17–19).

All the reflection traveltimes were fitted to within a 240-ms root-mean-square static shift (measured at the center of each reflection). The reflection-moveout variation was fitted to within an 80-ms root-mean-square error (measured from end to end); the spread in moveout versus azimuth in figure 17 is the result of a two-dimensional projection of varying shot-receiver geometry and velocity variations. These errors are less than the uncertainties inherent in the three-dimensional velocity model that we apply (370 ms; Parsons and Zoback, 1997). The fits to the reflections shown in figures 15 through 18, and the depth points shown in figure 19 were made by using the three-dimensional model. The collective moveout observations constrain a range in dip from 55º to 62º, with the best fit at 60º.

Repeated reflection observations at different offset ranges provide the overlapping depth coverage that limits possible solutions. The sources identified in figure 14 in San Francisco Bay represent groups of airgun shots ranging from at least 5 to 20 sequential reflection observations. Thus, although 37 modeled source points are marked in figure 14 (dots), actually hundreds of repeated observations were made. The airgun spacing was ~100 m, generating only slight variations in reflection time and moveout between adjacent shots; however, the repeated sequential reflection observations give us confidence in their validity. The distribution in source-receiver locations produces reflection depth points on the 60º-NE.-dipping structure along the strike of much of the San Andreas Fault, from the north at Bolinas Lagoon to the south at the city of San Mateo, a distance of 50 km (fig. 14). The depth coverage on the dipping structure ranges from 14 to 22 km (fig. 19*B*). This dipping horizon passes beneath a right step in the San Andreas Fault where the M=7.8 1906 San Francisco earthquake is thought to have initiated offshore of San Francisco (Zoback and others, 1999). We model this right step as a slight bend in the fault at depth (fig. 16).

We similarly model a separate group of southwest-dipping reflections from beneath San Francisco Bay (fig. 14). Among the 37 groups of airgun and explosive sources shown in figures 14 through 16, 13 produced reflections from a 70º-SW.-dipping structure between 22- and 24-km depth paralleling the Hayward Fault east of San Francisco Bay (figs. 14, 19). We observe this dipping structure from north of the city of Berkeley to south of the city of Hayward, an along-strike distance of 34 km (fig. 14). The combined land and marine depth coverage ranges from 18 to 24 km. The Hayward Fault predates the Peninsular segment of the San Andreas Fault, has more cumulative slip (50–70 versus 19–23 km; Cummings, 1968; McLaughlin and others, 1996), and appears to dip more steeply beginning deeper in the crust.

Virtually all of the coherent high-amplitude reflections recorded beneath San Francisco Bay at near-vertical incidence have thus been fitted to dipping structures associated with either the San Andreas or Hayward Fault. No continuous high-amplitude horizontal reflections were observed from the Moho or the top of the lower crust, although weaker, discon-

tinuous events were observed on some gathers that might be from lower-angle horizons beneath the bay at 15- to 25-km depth.

Integration, Implications, and Conclusions

The impetus for conducting seismic experiments in the San Francisco Bay region was to test several tectonic models that postulated the existence of lower-angle, linking faults in the midcrust to lower crust. To explain the observed heat flow, crustal structure, surface compressional features, and offshore magnetic anomalies, various workers have proposed a low-angle mechanical link in the lower crust or midcrust that extends between the San Andreas and Hayward Faults or across both (for example, Furlong and others, 1989; Furlong, 1993; Page and Brocher, 1993; Brocher and others, 1994; Jones and others, 1994; Bohannon and Parsons, 1995). The depth to which high-angle strike-slip faults penetrate is important in resolving the possible interaction between faults beneath seismogenic depths (Furlong and others, 1989) and how much strain localizes in fault zones (for example, Sanders, 1990).

Our interpretation of the collective results from seismic studies in the San Francisco Bay region is that no low-angle detachment fault is required between the major strike-slip faults to balance seismogenic strain. Together, the results from active- and passive-source seismic studies in the San Francisco Bay region show shallow and deep crust that is dominated by slip along high-angle to vertical strike-slip faults. Evidence from turning rays and refractions, as well as direct reflections, indicates that the strike-slip faults pierce the entire crust. Also, geodetic and earthquake measurements indicate that lower-crustal slip occurs on the San Andreas Fault (for example, King and others, 1987; Sanders, 1990). Crustal-velocity models across the San Andreas Fault near the Mendocino triple junction (Henstock and others, 1997) and in San Francisco Bay near the Golden Gate (Holbrook and others, 1996) show evidence for upper-mantle offset or lower-crustal velocity anomalies associated with near-vertical strike-slip faults. If the major strike-slip faults of the San Francisco Bay region do penetrate the whole crust, then the implication is that broadly distributed viscoelastic strain in the lower crust or strain occurring on low-angle structures is minimized. Thus, the primary link between the faults may be stress transfer through the elastic crust (for example, Stein and Lisowski, 1983; Reasenberg and Simpson, 1992).

An integration of seismic-reflection and seismicity data at the Kirby Hills fault zone provide evidence for high-angle (~80° dip) faulting that extends from the surface downward

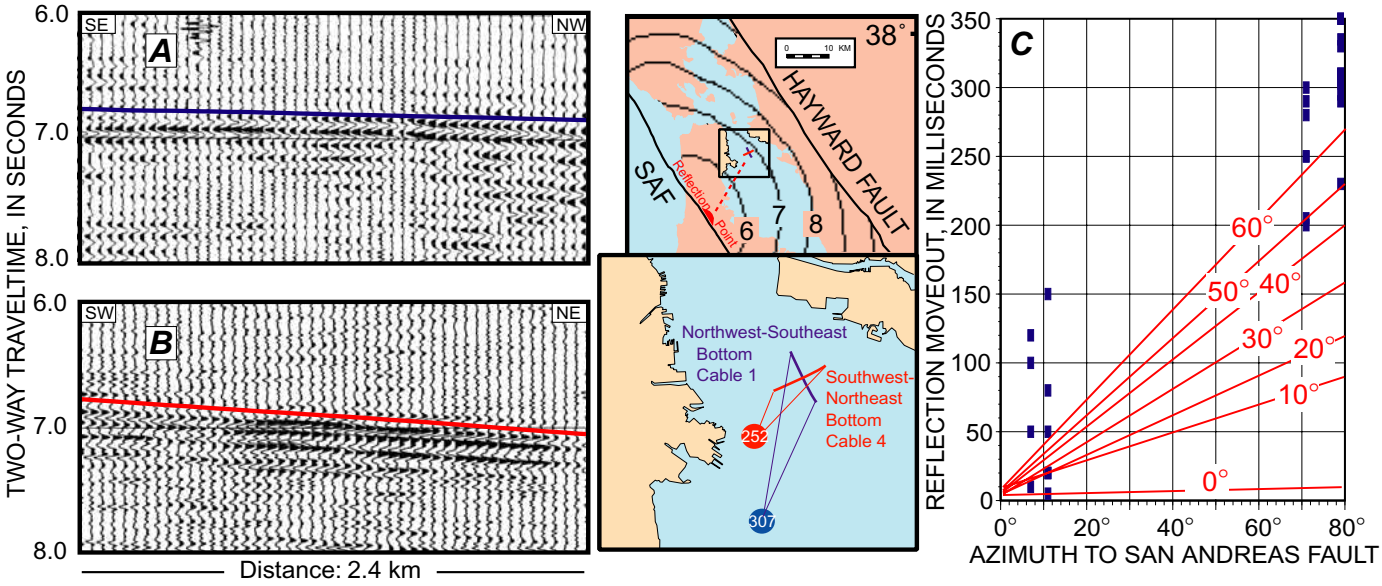

Figure 17.—Example reflections from two crossing bottom-cable profiles oriented parallel (*A*) and orthogonal (*B*) to strike of the San Andreas (SAF) and Hayward Faults. If these events reflected from a horizontal or low-angle impedance contrast, azimuth of recording cables would be unimportant, and both events would appear nearly flat. However, a strong dependence on receiver azimuth is noted: more than 200 ms greater moveout is observed on cable orthogonal to the San Andreas Fault than on that parallel to it, indicating that reflector dips down to northeast. Both arrivals are closely fitted by a 60°-NE.-dipping reflector that parallels the San Andreas Fault and begins at 12-km depth. Maps show reflected traveltime contours from three-dimensional modeling (Hole and Zelt, 1995) of events; a two-dimensional cross-sectional view is shown in figure 19. *C*, Reflection moveout versus recording-cable azimuth with respect to the San Andreas Fault for all 33 modeled reflection gathers. Events with greatest moveout are observed on orthogonal cables. Expected moveout from various dips is plotted on observations. Spread in moveout observations results from this two-dimensional projection of a three-dimensional geometry that includes varying source-receiver offsets and local velocity changes. Root-mean-square misfit of three-dimensional moveout, 80 ms.

to approximately the base of the crust. Because first-motion studies of earthquakes along the Kirby Hills Fault indicate predominantly right-lateral strike-slip motion, we interpret this fault to be the easternmost strand of the San Andreas Fault system. As such, this structure is presently offsetting the Cretaceous-Tertiary Coast Range-Great Valley tectonic wedge. The presence of whole-crustal dextral strike-slip faulting along the Coast Range-Great Valley boundary suggests that at this latitude, tectonic wedging is not currently active. Instead, any tectonic wedge that may have been constructed in the past is now being sliced and dismembered along the near-vertical crust-penetrating fault system at the east edge of the Coast Ranges.

The San Andreas and Hayward Faults are also modeled as cutting through the whole crust, at moderate to steep dip (60º–70º). If the interpreted lower-crustal dips of the San Andreas and Hayward Faults persist beneath the crust, these two faults would intersect at ~45-km depth, 20 km into the upper mantle (fig. 19). Below that depth, a single fault might accommodate all the relative Pacific-North American Plate motion. Our observations of fault-plane reflections are limited to crustal depths because the constraints of marine recording in San Francisco Bay prohibit the long source-receiver offsets required to observe deeper, dipping reflections. We can thus only speculate about the sub-Moho geometry of the faults (fig. 19). The dip of the faults might change after crossing the rheologic boundary at the Moho; the initiation of fault dip appears to be related to layer boundaries (seismic-velocity steps), identified by wide-angle seismic methods, that also represent rheologic boundaries (Holbrook and others, 1996). Thus, a lower-angle fault might still be present in the upper mantle (fig. 19), although we observe no reflections from any near-horizontal boundaries at later traveltimes that could be observed at near offsets. Interestingly, all the faults identified in the lower crust of the San Francisco Bay region have some apparent dip, ranging from ~60º on the San Andreas Fault to ~80º on the Kirby Hills Fault.

The relatively high amplitude (~5 dB above background) of reflections from deep, dipping surfaces signifies strong impedance contrasts in the lower crust beneath the surface traces of the Hayward and San Andreas Faults. Thus, right-lateral movement on these faults may have occurred through the whole crust and offset significantly different rock types. Alternatively, the presence of fluids in the fault zones or localized shearing and accompanying metamorphism within the fault zones may have generated an impedance contrast (for example, Fountain and others, 1984; Wang and others, 1989; Kern and Wenk, 1990; Siegesmund and others, 1991).

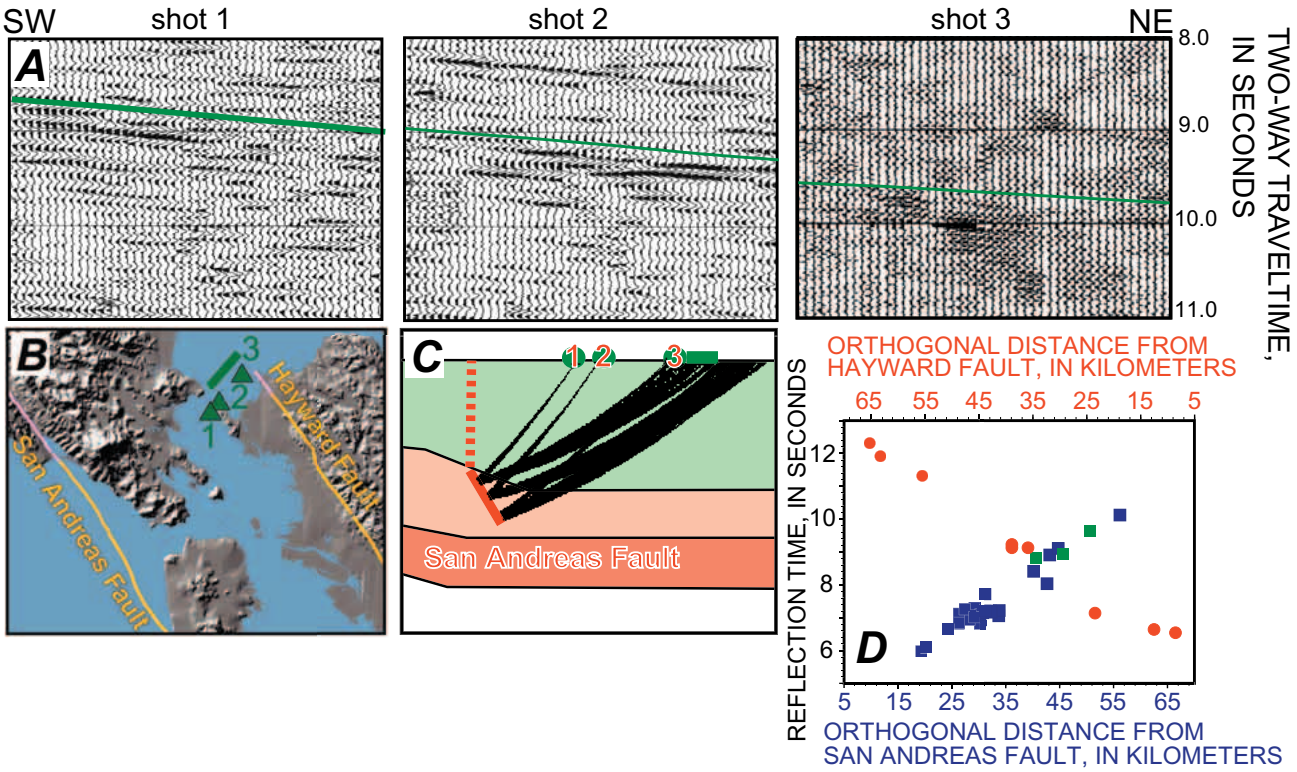

Figure 18.—Three shot gathers (*A*) recorded in northern San Francisco Bay (*B*), each showing same reflection event from the San Andreas Fault. Traveltime is progressively later with increasing shot distance northeast of fault, a consequence of a dipping reflector (*C*). Calculated three-dimensional reflection traveltimes from a 60° modeled reflector are superimposed on data plots. *D*, Reflection times to center of all modeled reflections as a function of their distance from the San Andreas (blue squares) or Hayward (red dots) Fault. Those source-receiver pairs located farthest from faults have reflections with latest arrivals. Three green squares represent data examples shown in figure 18*A*.

The typical width in time of the high-amplitude reflections and coda is ~1 s. Given the uncertainties of potential near-surface reverberations and along-path scattering, we cannot comment on the width or possible multilayering of the reflectors, although the high reflection amplitudes suggest a possible fluid-saturated zone (for example, Brown and others, 1987).

We note that the results collected here do not dispute the previous observation of a regional high-velocity layer at long source-receiver offsets (Brocher and others, 1994; Holbrook and others, 1996). Wide-angle reflections can be returned from a velocity gradient that is transparent at near-vertical incidence. Our results do show that the higher resolution, near-vertical-incidence reflections do not correspond to the top of the high-velocity, mafic composition, lower-crustal layer, as previously interpreted.

Acknowledgments

We thank Richard Allen, Peter Barnes, Bob Bohannon, Tom Burdette, Philip Burrows, Sam Clarke, Diana Collins, Ed Criley, Lynn Dietz, Moritz Fliedner, Anne Gibbs, Niki Godfrey, Mike Hamer, Jason Kelley, Will Kohler, Björn Lund, Richard Marsden, Andy Michael, Janice Murphy, Jean Olson, Stephanie Ross, David Rutledge, Holly Ryan, and George Thompson for their help in gathering the onland seismic-reflection data. The Golden Gate National Recreation Area, the Crystal Springs Water District, and the San Francisco Public Utilities Commission kindly permitted access to restricted lands. Seismic recording instruments and support were provided by the Incorporated Research Institutions for Seismology and Program for Array Seismic Studies of the Continental Lithosphere; Marcos Alvarez, Simon Klemperer, Bill Koperwhats, Steve Michnick, and Anthony Wei, Tom Burdette, John Coakley, Jason Kelley, Gonzalo Mendoza, Jean Olsen, and David Rutledge were indispensable during the acquisition and reduction of local network data. Tom Brocher, Rufus Catchings, and Steve Holbrook provided traveltime picks from their San Francisco Bay region controlled-source seismic experiments. Jon Childs, Dave Hogg, Walt Olson, Kevin O'Toole, Hal Williams, and Bill Robinson provided innovative solutions to difficult marine operational

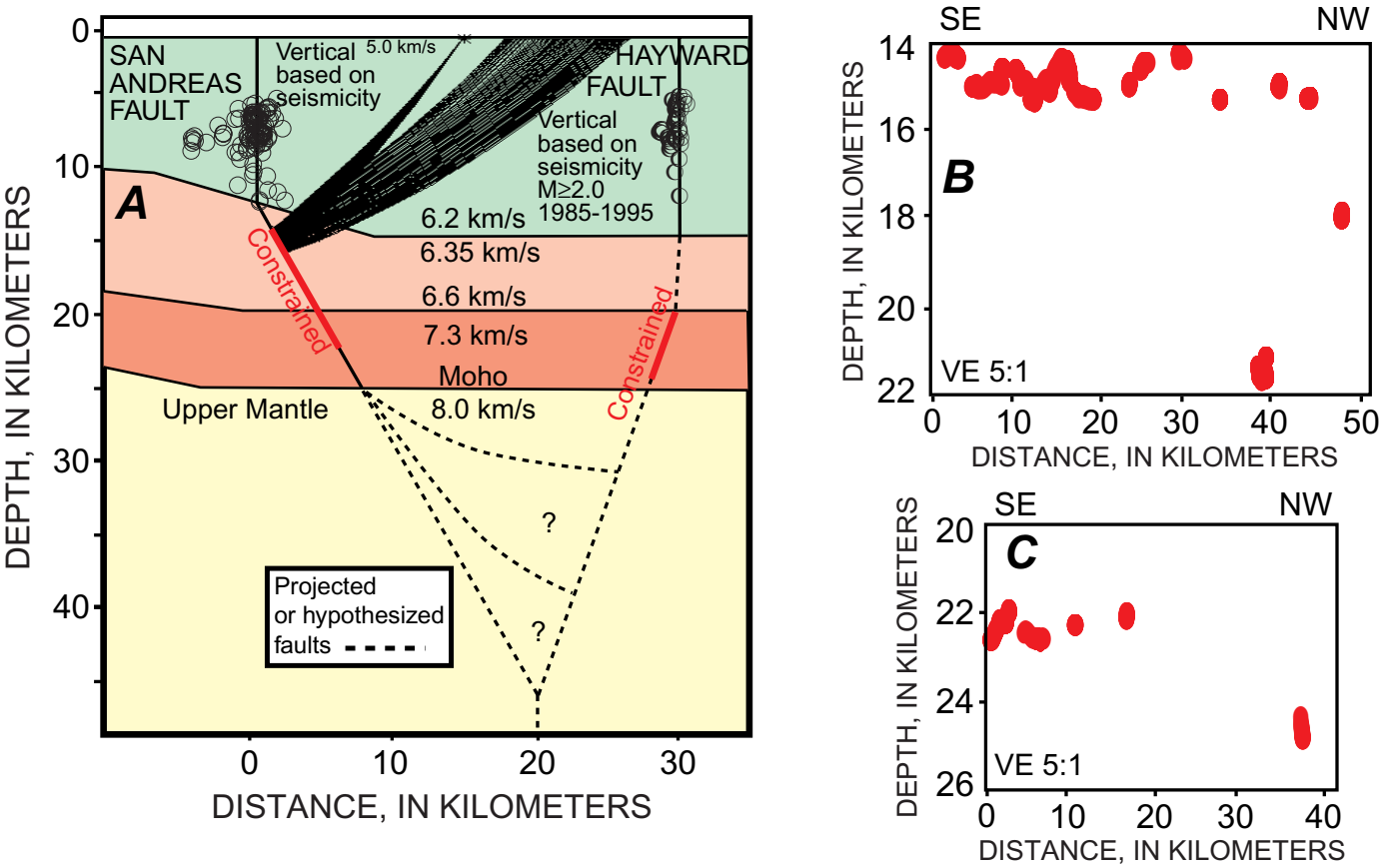

Figure 19.—Reflection modeling of the San Andreas and Hayward Faults. *A*, Cross-sectional view. Earthquake hypocenters show that faults are near vertical in uppermost ~12 km of crust. Red fault planes, depth extent that reflections from them are modeled; dashed lines, projected and conjectural relation between the two faults in upper mantle. *B*, Subsurface reflection-depth-point coverage on the San Andreas Fault, projected onto two-dimensional plane associated with segments identified in figure 1. *C*, Subsurface reflection-depth-point coverage on the Hayward Fault. Points represent only 37 modeled gathers; complete data coverage is more continuous. Three-dimensional model planes have a constant dip but bend where vertical parts of faults bend.

situations. Discussions with Kevin Furlong, Bob Jachens, Art Lachenbruch, Ben Page, and George Thompson helped to guide our thinking. Guy Cochrane, Alan Cooper, and Eric Geist reviewed the manuscript, which was edited by George Havach.

References Cited

Addicott, W.O., 1969, Late Pliocene mollusks from San Francisco Peninsula, California, and their paleogeographic significance: California Academy of Sciences Proceedings, ser. 4, v. 37, no. 3, p. 57–93.

Bakun, W.H., 1999, Seismic activity of the San Francisco Bay region: Seismological Society of America Bulletin, v. 89, no. 3, p. 764–784.

Beaudoin, B.C., 1994, Lower-crustal deformation during terrane dispersion along strike-slip faults: Tectonophysics, v. 232, no. 1–4, p. 257–266.

Blake, M.C., Jr., 1984, Franciscan geology of northern California: Society of Economic Paleontologists and Mineralogists, Pacific Section Field Trip Guidebook, v. 43, 254 p.

Bohannon, R.G., and Parsons, Tom, 1995, Tectonic implications of post-30 Ma Pacific and North American relative plate motions: Geological Society of America Bulletin, v. 107, no. 8, p. 937–959.

Brabb, E.E., and Pampeyan, E.H., compilers, 1983, Geologic map of San Mateo County, California: U.S. Geological Survey Miscellaneous Investigations Series Map I–1257–A, scale 1:62,500.

Brocher, T. M., McCarthy, Jill, Hart, P.E., Holbrook, W.S., Furlong, K.P., McEvilly, T.V., Hole, J.A., and Klemperer, S.L., 1994, Seismic evidence for a lower-crustal detachment beneath San Francisco Bay, California: Science, v. 265, no. 5177, p. 1436–1439.

Brocher, T.M., and Moses, M.J., 1993, Onshore-offshore wide-angle seismic recordings of the San Francisco Bay area seismic imaging experiment (BASIX); the five-day recorder data, U.S. Geological Survey Open-File Report 93–276, 89 p.

Brocher, T.M., and Pope, D.C., 1994, Onshore-offshore wide-angle seismic recordings of the San Francisco Bay Area seismic imaging experiment (BASIX); data from the Northern California Seismic Network: U.S. Geological Survey Open-File Report 94–156, 123 p.

Brown, L.D., Wille, C.E., Zheng, Li, de Voogd, Beatrice, Mayer, J.R., Hearn, T.M., Sanford, W.E., Caruso, C.W., Zhu, T.F., Nelson, D.K., Potter, C.J., Hauser, E.C., Klemperer, S.L., Kaufman, Sidney, and Oliver J.E., 1987, COCORP; new perspectives on the deep crust: Royal Astronomical Society Geophysical Journal, v. 89, no. 1, p. 47–54.

Bürgmann, Roland, 1997, Active detachment faulting in the San Francisco Bay area?: Geology, v. 25, no. 12, p. 1135–1138.

Catchings, R.D., and Kohler, W.M., 1996, Reflected seismic waves and their effect on strong shaking during the 1989 Loma Prieta, California, earthquake: Seismological Society of America Bulletin, v. 86, no. 5, p. 1401–1416.

Cummings, J.C., 1968, The Santa Clara Formation and possible post-Pliocene slip on the San Andreas fault in central California, *in* Dickinson, W.R., and Grantz, Art, eds., Proceedings of the conference on geologic problems of the San Andreas fault system: Stanford, Calif., Stanford University Publications in Geological Sciences, v. 11, p. 191–207.

DeMets, Charles, Gordon, R.G., Argus, D.F., and Stein, Seth, 1990, Current plate motions: Geophysical Journal International, v. 101, no. 2, p. 425–478.

Dewey, J.W., Hill, D.P., Ellsworth, W.L., and Engdahl, E.R., 1989, Earthquakes, faults, and the seismotectonic framework of the contiguous United States, *in* Pakiser, L.C., and Mooney, W.D., eds., Geophysical framework of the continental United States: Geological Society of America Memoir 172, p. 541–576.

Fountain, D.M., Hurich, C.A., and Smithson, S.B., 1984, Seismic reflectivity of mylonite zones in the crust: Geology, v. 12, no. 4, p. 195–198.

Furlong, K.P. 1993, Thermal-rheologic evolution of the upper mantle and the development of the San Andreas fault system: Tectonophysics, v. 223, no. 1–2, p. 149–164.

Furlong, K.P., Hugo, W.D., and Zandt, George, 1989, Geometry and evolution of the San Andreas fault zone in northern California: Journal of Geophysical Research, v. 94, no. B3, p. 3100–3110.

Hall, N.T., 1984, Holocene history of the San Andreas fault between Crystal Strings Reservoir and San Andreas Dam, San Mateo County, California: of the Seismological Society of America Bulletin, v. 74, no. 1, p. 281–299.

Hall, N.T., and Wright, R.H., 1993, Paleoseismic investigations of the San Andreas Fault on the San Francisco Peninsula, California: final technical report to U.S. Geological Survey, National Earthquake Hazards Reduction Program, 15 p.

Hall, N.T., Wright, R.H., Clahan, K.B., 1996, Paleoseismic investigations of the San Andreas fault on the San Francisco Peninsula, California: Reston, Va., U.S. Geological Survey, National Earthquake Hazards Reduction Program Final Technical Report 14–08–0001–G2081, 45 p.

Henstock, T.J., Levander, A.R., and Hole, J.A., 1997, Deformation in the lower crust of the San Andreas fault system in northern California: Science, v. 278, no. 5338, p. 650–653.

Hill, D.P., Eaton, J.P., and Jones, L.M., 1990, Seismicity, 1980–86, chap. 5 *of* Wallace, R.E., ed., The San Andreas fault system, California: U.S. Geological Survey Professional Paper 1515, p. 115–151.

Holbrook, W.S., Brocher, T.M., ten Brink, U.S., and Hole, J.A., 1996, Crustal structure of a transform plate boundary, San Francisco Bay and the central California continental margin: Journal of Geophysical Research, v. 101, no. B10, p. 22311–22334.

Hole, J.A., 1992, Nonlinear high-resolution three-dimensional seismic travel time tomography: Journal of Geophysical Research, v. 97, no. B5, p. 6553–6562.

Hole, J.A., Klemperer, S.L., Brocher, T.M., Parsons, Tom, Benz, H.M., and Furlong, K.P., 2000, Three-dimensional seismic velocity structure of the San Francisco Bay area: Journal of Geophysical Research, v. 105, no. B6, p. 13859–13874.

Hole, J.A., and Zelt, B.C., 1995, 3-D finite-difference reflection traveltimes: Geophysical Journal International, v. 121, no. 2, p. 427–434.

Jones, D.L., Graymer, R.W., Wang, Chi, McEvilly, T.V., and Lomax, Anthony, 1994, Neogene transpressive evolution of the California Coast Ranges: Tectonics, v. 13, no. 3, p. 561–574.

Kelson, K.I., Lettis, W.R., and Lisowski, Michael, 1992, Distribution of geologic slip and creep along faults in the San Francisco Bay region, *in* Galehouse, J.S., ed., Programs and abstracts of the second conference on earthquake hazards in the eastern San Francisco Bay area: California Division of Mines and Geology Special Publication 113, p. 31–38.

Kern, Hartmut, and Wenk, H.-R., 1990, Fabric-related velocity anisotropy and shear wave splitting in rocks from the Santa Rosa mylonite zone, California: Journal of Geophysical Research, v.

95, no. B7, p. 11213–11223.
King, N.E., Segall, Paul, and Prescott, W.H., 1987, Geodetic measurements near Parkfield California, 1959–1984: Journal of Geophysical Research, v. 92, no. B3, p. 2747–2766.
Kohler, W.M., and Catchings, R.D., 1994, Data report for the 1993 seismic refraction experiment in the San Francisco Bay area, California: U.S. Geological Survey Open-File Report 94–241, 71 p.
Krug, E.H., Cherven, V.B., Hatten, C.W., and Roth, J.C., 1992, Subsurface structure in the Montezuma Hills, southwestern Sacramento Basin, *in* Cherven, V.B., and Edmondson, W.F., eds., Structural geology of the Sacramento Basin: American Association of Petroleum Geologists, Pacific Section Miscellaneous Publication 41, p. 41–60.
Lisowski, Michael, Savage, J.C., and Prescott, W.H., 1991, The velocity field along the San Andreas fault in central and southern California: Journal of Geophysical Research, v. 96, no. B5, p. 8369–8389.
Marlow, M.S., Jachens, R.C., Hart, P.E., Carlson, P.R., Anima, R.J., and Childs, J.R., 1999, Development of San Leandro Synform and neotectonics of the San Francisco Bay Block, California: Marine and Petroleum Geology, v. 16, no. 5, p. 431–442.
McCarthy, Jill, and Hart, P.E., 1993, Data report for the 1991 Bay area seismic imaging experiment (BASIX): U.S. Geological Survey Open-File Report 93–301, 26 p.
McKevett, N.H., 1992, The Kirby Hills fault zone, *in* Cherven, V.B., and Edmondson, W.F., eds., Structural geology of the Sacramento Basin: American Association of Petroleum Geologists, Pacific Section Miscellaneous Publication 41, p. 61–78.
McLaughlin, R.J., Sliter, W.V., Sorg, D.H., Russell, P.C., and Sarna-Wojcicki, A.M., 1996, Large-scale right-slip displacement on the East San Francisco Bay region fault system, California; implications for location of late Miocene to Pliocene Pacific plate boundary: Tectonics, v. 15, no. 1, p. 1–18.
Murphy, J.M., Catchings, R.D., Kohler, W.M., Fuis, G.S., and Eberhart-Phillips, D.M., 1992, Data report for 1991 active-source seismic profiles in the San Francisco Bay area, California: U.S. Geological Survey Open-File Report 92–570, 45 p.
Olson, J.A., and Lindh, A.G., 1985, Seismicity of the San Andreas Fault from Cienega Winery to the Golden Gate, *in* Shearer, C.F., ed., Minutes of the National Earthquake Prediction Evaluation Council, July 26–27, 1985, Menlo Park, California: U.S. Geological Survey Open-File Report 85–754, p. 316–324.
Olson, J.A., and Zoback, M.L., 1992, Seismic deformation patterns on the San Francisco peninsula [abs.]: Eos (American Geophysical Union Transactions), v. 73, no. 43, supp., p. 401.
Page, B.M., 1992, Tectonic setting of the San Francisco Bay Region, *in* Galehouse, J.S., ed., Programs and abstracts of the second conference on earthquake hazards in the eastern San Francisco Bay area: California Division of Mines and Geology Special Publication 113, p. 1–7.
Page, B.M., and Brocher, T.M., 1993, Thrusting of the central California margin over the edge of the Pacific plate during the transform regime: Geology, v. 21, no. 7, p. 635–638.
Parsons, Tom, 1998, Seismic reflection evidence that the Hayward fault extends into the lower crust of the San Francisco Bay area: Seismological Society of America Bulletin, v. 88, no. 5, p. 1212–1223.
Parsons, Tom, and Hart, P.E., 1999, Dipping San Andreas and Hayward faults revealed beneath San Francisco Bay, California: Geology, v. 27, no. 9, p. 839–842.
Parsons, Tom, and Zoback, M.L., 1997, Three dimensional upper crustal velocity structure beneath San Francisco Peninsula, California: Journal of Geophysical Research, v. 102, no. B3, p. 5473–5490.
Reasenberg, P.A., and Simpson, R.W., 1992, Response of regional seismicity to the static stress change produced by the Loma Prieta earthquake: Science, v. 255, no. 5052, p. 1687–1690.
Ross, D.C., 1978, The Salinian Block; Mesozoic granite orphan in the California Coast Ranges, *in* Howell, D.G., and McDougall, K.A., eds., Mesozoic paleogeography of the Western United States (Pacific Coast Paleogeography Symposium 2): Los Angeles, Society of Economic Paleontologists and Mineralogists, Pacific Section, p. 509–522.
Sanders, C.O., 1990, Earthquake depths and the relation to strain accumulation and stress near strike-slip faults in southern California: Journal of Geophysical Research, v. 95, no. B4, p. 4751–4762.
Siegesmund, Sigfried, Fritzsche, Michael, and Braun, Günther, 1991, Reflectivity caused by texture-induced anisotropy in mylonites, *in* Meissner, R.O., Brown, L.D., Dürbaum, H.-J., Franke, Wolfgang, Fuchs, Karl, and Seifert, Friedrich, eds., Continental lithosphere; deep seismic reflections (Geodynamics Series, v. 22): Washington D.C., American Geophysical Union, p. 291–298.
Stanley, W.D., Benz, H.M., Walters, M.A., Villaseñor, Antonio, and Rodriguez, B.D., 1998, Tectonic controls on magmatism in The Geysers-Clear Lake region; evidence from new geophysical models: Geological Society of America Bulletin, v. 110, no. 9, p. 1193–1207.
Stein, R.S., and Lisowski, Michael, 1983, The 1979 Homestead Valley earthquake sequence, California; control of aftershocks and postseismic deformation: Journal of Geophysical Research, v. 88, no. B8, p. 6477–6490.
Taylor, C.L., Cummings, J.C., and Ridley, A.P., 1980, Discontinuous en echelon faulting and ground warping, Portola Valley, California, *in* Streitz, Robert, and Sherburne, R.W., eds., Studies of the San Andreas fault zone in northern California: California Division of Mines and Geology Special Report 140, p. 59–70.
Thatcher, Wayne, 1975, Strain accumulation and release mechanism of the 1906 San Francisco earthquake: Journal of Geophysical Research, v. 80, no. 35, p. 4862–4872.
Thurber, C.H., 1993, Local earthquake tomography; velocities and V_p/V_s—theory, *in* Iyer, H.M., and Hirahara, Kazuro, eds., Seismic tomography; theory and practice: London, Chapman and Hall, p. 663–683.
Vidale, J.E., 1990, Finite-difference calculation of traveltimes in three dimensions: Geophysics, v. 55, no. 5, p. 521–526.
Wakabayashi, John, and Moores, E.M., 1988, Evidence for collision of the Salinian block with the Franciscan subduction zone, California: Journal of Geology, v. 96, no. 2, p. 245–253.
Wang, Chi, Okaya, D.A., Ruppert, Charles, Davis, G.A., Guo, Tieshuan, Zhong, Zengqui, and Wenk, H.-R., 1989, Seismic reflectivity of the Whipple Mountain shear zone in southern California: Journal of Geophysical Research, v. 94, no. B3, p. 2989–3005.
Zoback, M.L., Jachens, R.C., and Olson, J.A., 1999, Abrupt along-strike change in tectonic style; San Andreas fault zone, San Francisco Peninsula: Journal of Geophysical Research, v. 104, no. B5, p. 10719–10742.